

Dynamic Modularity Approach to Adaptive Inner/Outer Loop Control of Robotic Systems

Hanlei Wang, Wei Ren, Chien Chern Cheah, and Yongchun Xie

Abstract—Modern applications of robotics typically involve a robot control system with an inner PI (proportional-integral) or PID (proportional-integral-derivative) control loop and an outer user-specified control loop. The existing outer loop controllers, however, do not take into consideration the dynamic effects of robots and their effectiveness relies on the ad hoc assumption that the inner PI or PID control loop is fast enough (generally impossible in practice), and other torque-based control algorithms cannot be implemented in robotics with closed architecture (i.e., the torque control loop is closed). This paper investigates the adaptive control of robotic systems with an inner/outer loop structure, taking into full account the effects of the dynamics and the system uncertainties, and both the task-space control and joint-space control are considered. We propose a dynamic modularity approach to resolve this issue, and a class of adaptive outer loop control schemes is proposed and their role is to dynamically generate the joint velocity (or position) command for the low-level joint servoing loop. Without relying on the ad hoc assumption that the joint servoing is fast enough or the modification of the low-level joint controller structure, we rigorously show that the proposed outer loop controllers can ensure the stability and convergence of the closed-loop robotic system. We also propose the outer loop versions of several standard direct/composite adaptive joint-space controllers for rigid robots or flexible-joint robots, and a promising conclusion may be that most torque-based adaptive controllers for robots can be designed to fit the inner/outer loop structure by using the new definition of the joint velocity (or position) command based on the adaptively scaled dynamic compensation. Simulation results are provided to show the performance of various adaptive outer loop controllers, using a three-DOF (degree-of-freedom) manipulator.

Index Terms—Inner/outer loop, adaptive control, dynamic modularity approach, robotics.

I. INTRODUCTION

User-friendliness is an important aspect of modern automatic machines, especially if they are expected to do extensive work in cooperation with human beings. The control systems for modern robotic systems, unfortunately, have not yet reach this expectation though numerous control algorithms have been developed over the past several decades. To serve this purpose, the controlled robotic system might have to be reliable, robust, and flexible to satisfy the user's needs. As we take a deep look at the development of computers (for instance, the recent hybrid computers—Surface Pro 4, iPad Pro, etc.), the module design plays a vital role in promoting their success in our everyday life. The relationship between the operating systems (e.g., the Windows System) and the application programs further validates the desirability of this module design philosophy.

Historically, the applications of robotics have undergone the following phases:

- 1) Traditional industrial applications—factory automation in a structured environment with a simple joint-space PID

H. Wang is with the Science and Technology on Space Intelligent Control Laboratory, Beijing Institute of Control Engineering, Beijing 100094, China (e-mail: hlwang.bice@gmail.com).

W. Ren is with the Department of Electrical and Computer Engineering, University of California, Riverside, CA 92521 USA (e-mail: ren@ee.ucr.edu).

C. C. Cheah is with the School of Electrical and Electronic Engineering, Nanyang Technological University, Singapore 639798, Republic of Singapore (e-mail: ecccheah@ntu.edu.sg).

Y. Xie is with the Science and Technology on Space Intelligent Control Laboratory, Beijing Institute of Control Engineering, Beijing 100094, China (e-mail: xieyongchun@vip.sina.com).

(proportional-integral-derivative) inner loop control as well as inverse kinematics;

- 2) Modern applications—beyond factory automation in an unstructured environment with sensory feedback in the task space, e.g., (outer loop) visual servoing and task-space control, which, however, either cannot be implemented in robotics with closed architecture or rely on the ad hoc assumption that the combination of the inner and outer loops is stable and the effect of the dynamics can be neglected. This ad hoc assumption typically (approximately) holds only on the occasion that the given task is slow enough.

The inner/outer loop structure of robotic systems (e.g., most commercial robotic systems) enjoys certain module design flavor and has some desirable properties, e.g., it is beneficial for generating a high joint stiffness by employing a fast inner joint servoing while it is not reliable as directly specifying the control torque due to the limitation of the communication (generally required for exerting a coupling control action) reliability. For this reason, the gap between the study of advanced robot control theory and practical applications is longstanding. In the academic field, most advanced controller designs are torque-based and typically require an open torque control loop. In practical applications, the much more reliable and robust velocity control mode is adopted. It seems necessary here to recall the standard inner/outer loop structure of most commercial (industrial) robotic systems: 1) an outer (kinematic) loop using a centralized computer with enough computing power; 2) an inner dynamic loop that consists of n independent processors equipped at each joint in a decentralized way (i.e., each processor only receives/sends signals from/to its local sensors, actuator, and the centralized computer). The inner dynamic loop usually evolves at a much faster sampling than the outer (kinematic) loop.

The attempts that aim to address the control of this kind of robotic systems in the task space occur in, e.g., [1], [2], [3], [4]. However, these controllers cannot ensure the tracking error convergence without significantly modifying the low-level PI (proportional-integral) controller to be a more complex one. One may note that these control algorithms are all based on the standard resolved motion rate control proposed by [5] to design the joint velocity command. Then what actually prevents the application of advanced robot controllers? Let us first retrospect the realization of the standard computed torque controller that has been discussed in [6, p. 209, p. 210] (see also the trajectory precompensation based on the computed torque feedforward in [7]). The specific procedure in [6] is to modify the terms in the feedforward action that may involve coupling by replacing certain signals (positions or velocities) with their desired values. In this way, no communication between the joint processors at the dynamic servoing loop is required since the desired values of all the joints are stored in each joint's computer a priori (which would, on the other hand, mean that this algorithm is not flexible in the case that the desired trajectory is subjected to changes). The overall impression is that for the sake of reducing computational burden, this scheme performs the feedforward at the joint control loop in a relatively limited manner and with many nonlinear terms being neglected. Another important well-recognized reason is that most commercial/industrial robotic systems do not have an open torque control loop (see, e.g., [8]). These two factors give rise to the awkward situation of the modern torque-based robot control algorithms (e.g., the adaptive algorithms in [9], [10], [11], [12], [13], [14], [15] and the robust algorithms in [16], [17]), i.e., it is hard to apply these algorithms to robotic systems with an inner/outer loop structure. The precompensation scheme in [7], by producing a trajectory correction term based on the inverse manipulator dynamics and then adding it to the desired joint

trajectory, improves the performance of the industrial robotic system without modifying the low-level controller structure. The main proofs of the performance improvement, however, are by the experimental results rather than by the rigorous analysis.

In this paper, we rigorously address this issue in the context of adaptive task-space/joint-space control for robotic systems with an embedded low-level PI joint velocity controller (or PID joint position controller) and with uncertain dynamics (and kinematics). The use of PI velocity controller or PID position controller in most industrial/commercial robotic systems is well recognized (see, e.g., [18], [19]). Our main purpose here is to develop a class of adaptive outer loop controllers that can ensure the stability and convergence of the robotic systems with the dynamic effect being taken into full account and without modifying the embedded inner PI or PID control loop. The application of the current adaptive (or robust) task-space regulation/tracking algorithms (e.g., [20], [21], [12], [13], [15], [22], [23], [14], [24], [25]) to robotic systems with an inner/outer loop structure, for a long period, relies on the ad hoc assumption that the inner joint servoing loop is fast enough or the modification of the inner joint controller structure.

We first propose two adaptive task-space regulation controllers that rule out the fundamental limitations of the existing results, by dynamically incorporating an adaptively scaled dynamic compensation that exploits the physically independent nature of the low-level controller structure. The first controller, by introducing an adaptive filter, avoids the task-space velocity measurement, and the second one avoids the use of the task-space velocity by using an observer [motivated by the one in [26] with a modified feedback gain (which depends on the estimated Jacobian matrix) to achieve feedback separation]. Both of the adaptive controllers are qualified outer loop control schemes that can be applied to robotic systems with an unmodifiable joint servoing controller (PI velocity or PID position controller) (e.g., most industrial/commercial robots), taking into account the dynamic loop of the robotic systems. From a robot control perspective, most existing kinematic algorithms are not mathematically rigorous in that either the effects of the inner joint control loop are not considered (e.g., [27], [28], [29]), or the low-level joint servoing controller is assumed to be strong enough to ensure (yet cannot rigorously guarantee due to the absence of dynamic compensation action in the low-level dynamic loop) the square-integrability and boundedness of the velocity tracking error (e.g., [30], [31]), or even the modification of the low-level controller structure (e.g., [1], [2], [3]). These limitations are mainly caused by the inner/outer loop structure and closed controller architecture. The proposed outer loop controller here, by dynamically incorporating adaptively scaled dynamic compensation action and adaptive transpose Jacobian feedback, ensures the singularity-robust stability and convergence of the task-space position error without relying on any modification of the low-level PI/PID controller structure. Due to the independence of the design of the outer loop controller and that of the low-level PI/PID controller and the injection of the dynamic compensation, the proposed design approach is referred to as *dynamic modularity approach*.

We then show that the observer-based task-space regulation scheme can be extended to the case of task-space tracking. The obtained control scheme has an interesting feature that the inverse of the estimated Jacobian matrix is used for introducing feedforward and its transpose is used for introducing feedback, in contrast to most existing task-space algorithms that only employ the inverse of the Jacobian matrix to exert feedforward and feedback actions (see, e.g., [9], [32], [21], [14]), and the benefit of this lies in two folds: 1) it yields the feedback separation of the kinematic and dynamic loops, thus reducing the activity of the dynamic compensation action; 2) it

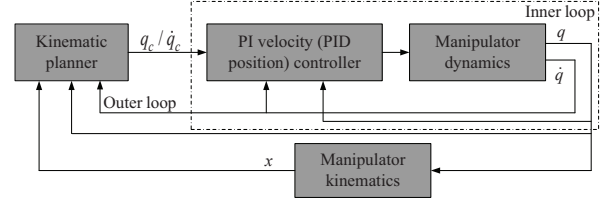


Fig. 1. Inner/outer loop control (q_c is the position command, \dot{q}_c is the velocity command, and q , \dot{q} , and x are the joint position, joint velocity, and task-space position, respectively).

is reducible in the sense that once the desired task-space velocity becomes zero, the tracking control law reduces to the regulation control law without involving the inverse of the estimated Jacobian matrix.

Finally, we illustrate how the adaptively scaled dynamic compensation enables several typical adaptive robot controllers for joint-space trajectory tracking to be applicable to robotic systems with an inner/outer loop structure (e.g., most industrial/commercial robotic systems). In particular, the proposed dynamic modularity approach is further shaped to incorporate the composite adaptation for improving performance and to address the issue of joint flexibility. By these additional examples, it seems hopeful that most adaptive dynamic controllers for robots in the literature with the use of adaptively scaled dynamic compensation and new definition of the joint velocity (or position) command would be rendered to be qualified outer loop schemes. Another potential favorable point may be the reduction of the cost of the laboratory experimental research on advanced robot control theory in that there no longer needs to develop a specific manipulator with an open torque control loop (usually requiring extensive efforts and time) and any commercial robot (cost-efficient due to the large-scale production) can be directly used.

II. PRELIMINARIES

A. Background and Motivation

Inner/outer loop control is typical in modern applications of robotic systems (see Fig. 1), and generally the inner loop is designed by the robot production company and closed and only the outer loop is open to the user. The user can specify the position or velocity command within the outer loop based on measurements in joint space [and task space (e.g., image space)], which is then sent to the inner loop as a reference signal. The main benefit of adopting an inner/outer loop structure may be that the inner loop (due to simplicity) can be operated at a high sampling rate and thus a high stiffness can be maintained, and that the outer loop can be operated at a low sampling rate allowing relatively complicated communication and sensing. In addition, inner/outer loop structure does help to realize the relative independence of the manipulator production company and the users, and to promote the large-scale production of manipulators due to the invariance of the inner control loop.

Historically, most theoretical results on adaptive manipulator control are presented in the context that the joint torque is directly designable rather than in the framework of the inner/outer loop. This results in the longstanding gap between the study of advanced robot control theory and the applications of robots. The existing results (e.g., [1], [2], [3], [7], [27], [28], [29]) are either ad hoc, e.g., effective under the assumption that the joint servoing is fast enough, relying on the modification of the low-level controller structure which is unmodifiable in practice, or not theoretically rigorous.

Our main purpose is to develop a class of adaptive outer loop controllers using the task-space and joint-space sensory measurement

(instead of obtaining the task-space information based on the kinematics as in Fig. 1 since the kinematics is unknown) to take place of the kinematic planner in Fig. 1 so that the stability and convergence of the closed-loop robotic systems with uncertain dynamics (and kinematics) can rigorously be ensured, and to finally approach the goal of “modularity”.

B. Manipulator Kinematics and Dynamics

Consider an n -DOF (degree-of-freedom) manipulator actuated by permanent magnet DC motors. Let $x \in R^m$ be the position of the end-effector in the task space and it is relevant to the joint position by the following nonlinear mapping [33], [34]

$$x = f(q) \quad (1)$$

where $q \in R^n$ denotes the joint position and $f : R^n \rightarrow R^m$ is the mapping from joint space to task space. We here assume that $n \geq m$, i.e., the manipulator can either be nonredundant or redundant.

Differentiating (1) with respect to time yields the relation between the task-space velocity \dot{x} and joint velocity \dot{q} [33], [34]

$$\dot{x} = J(q)\dot{q} \quad (2)$$

where $J(q) \in R^{m \times n}$ is the Jacobian matrix. If the kinematic parameters are unknown, the task-space position/velocity can no longer be derived by the direct kinematics given above. The typical practice in this case is to employ certain task-space sensors (e.g., a camera) to obtain the task-space position information.

The dynamics of the manipulator can be written as [34]

$$M(q)\ddot{q} + C(q, \dot{q})\dot{q} + B\dot{q} + g(q) = Ku \quad (3)$$

where $M(q) \in R^{n \times n}$ is the inertia matrix, $C(q, \dot{q}) \in R^{n \times n}$ is the Coriolis and centrifugal matrix, $B \in R^{n \times n}$ is a constant diagonal positive definite matrix, $g(q) \in R^n$ is the gravitational torque, $u \in R^n$ is the armature voltage, and $K \in R^{n \times n}$ is a constant diagonal positive definite matrix.

Four basic properties associated with (2) and (3) that shall be useful for the controller design and stability analysis are listed as follows.

Property 1 ([21]): The kinematics (2) depends linearly on a constant kinematic parameter vector a_k , which gives rise to

$$J(q)\psi = Y_k(q, \psi)a_k \quad (4)$$

where $\psi \in R^n$ is a vector and $Y_k(q, \psi)$ is the kinematic regressor matrix.

Property 2 ([35], [34]): The inertia matrix $M(q)$ is symmetric and uniformly positive definite.

Property 3 ([35], [34]): The matrix $C(q, \dot{q})$ can be appropriately defined such that the matrix $\dot{M}(q) - 2C(q, \dot{q})$ is skew-symmetric.

Property 4 ([35], [34]): The dynamics (3) depends linearly on a constant dynamic parameter vector a_d , which yields

$$M(q)\dot{\zeta} + C(q, \dot{q})\zeta + B\zeta + g(q) = Y_d(q, \dot{q}, \zeta, \dot{\zeta})a_d \quad (5)$$

where $\zeta \in R^n$ is a differentiable vector, $\dot{\zeta}$ is the time derivative of ζ , and $Y_d(q, \dot{q}, \zeta, \dot{\zeta})$ is the dynamic regressor matrix.

III. ADAPTIVE INNER/OUTER LOOP CONTROL

Kinematic control typically appears in the context of inner/outer loop control of robot manipulators and its focus is on the design of the joint velocity (or position) command. Historically, the effectiveness of kinematic control stands on the relatively strong assumption that the inner control (PI velocity control or PID position control) loop is fast enough so that the dynamic effects of the inner loop can be neglected. Here, we present a dynamic modularity approach to ensure

the convergence of the task-space position error, without relying on this ad hoc assumption or the modification of the inner control loop.

Let $x_d \in R^m$ denote the desired task-space position. For the regulation problem, it is set as constant; for the tracking problem, it can be set as time-varying and in this case, we assume that x_d , \dot{x}_d , and \ddot{x}_d are all bounded.

A. Filter-Based Adaptive Regulation Control

Consider the case that the inner control loop employs a PI velocity control, and the PI gains of the inner PI velocity control loop (the case of PID position control is discussed in Sec. III-D) are supposed to be K_P and K_I (diagonal and positive definite). Then, the PI action can be written as

$$u = -K_P(\dot{q} - \dot{q}_c) - K_I(q - q_c). \quad (6)$$

To avoid the task-space velocity measurement, we introduce the following adaptive passive filter

$$\dot{y} = -K_1 y + K_1 \hat{J}^T(q)\Delta x, \quad (7)$$

upon which, we define the joint reference velocity as

$$\dot{q}_r = -K_2 y \quad (8)$$

where $\Delta x = x - x_d$, K_1 and K_2 are diagonal positive definite matrices, and $\hat{J}(q)$ is the estimate of the Jacobian matrix $J(q)$ and is obtained by replacing a_k in $J(q)$ with its estimate \hat{a}_k . Define a sliding vector

$$s = \dot{q} - \dot{q}_r. \quad (9)$$

Substituting (8) into (2) and using Property 1 gives

$$\begin{aligned} \dot{x} &= -\hat{J}(q)K_2 y - [\hat{J}(q) - J(q)]\dot{q} - \hat{J}(q)\dot{q}_r + \hat{J}(q)\dot{q} \\ &= -\hat{J}(q)K_2 y - Y_k(q, \dot{q})\Delta a_k + \hat{J}(q)s. \end{aligned} \quad (10)$$

where $\Delta a_k = \hat{a}_k - a_k$.

We define the joint velocity command by the following dynamic system

$$\begin{aligned} \dot{q}_c + \hat{K}_I q_c &= \dot{q}_r + \hat{K}_I q_r + \text{diag}[\hat{w}_i, i = 1, \dots, n] \\ &\times \left[-\alpha \hat{J}^T(q)\Delta x + Y_d(q, \dot{q}, \ddot{q}_r)\hat{a}_d \right] \end{aligned} \quad (11)$$

with

$$q_r = q_r(0) + \int_0^t \dot{q}_r(\sigma) d\sigma \quad (12)$$

where $q_r(0)$ can be chosen as an arbitrary constant vector, α is a positive design constant, \hat{a}_d is the estimate of a_d , \hat{w}_i denotes the scale weight, $i = 1, \dots, n$, $\text{diag}[\hat{w}_i, i = 1, \dots, n][-\alpha \hat{J}^T(q)\Delta x + Y_d(q, \dot{q}, \ddot{q}_r)\hat{a}_d]$ denotes the adaptively scaled dynamic compensation action, and \hat{K}_I denotes the estimate of $K_I = K_P^{-1}K_I$, which can be expressed as

$$\hat{K}_I = \text{diag}[\hat{w}_I] \quad (13)$$

with \hat{w}_I being an n -dimensional vector. The adaptation laws for \hat{a}_k , $\hat{w} = [\hat{w}_1, \dots, \hat{w}_n]^T$, \hat{a}_d , and \hat{w}_I are given as

$$\dot{\hat{a}}_k = \Gamma_k Y_k^T(q, \dot{q})\Delta x \quad (14)$$

$$\dot{\hat{w}} = -\Lambda \text{diag}[-\alpha \hat{J}^T(q)\Delta x + Y_d(q, \dot{q}, \ddot{q}_r)\hat{a}_d]s \quad (15)$$

$$\dot{\hat{a}}_d = -\Gamma_d Y_d^T(q, \dot{q}, \ddot{q}_r, \ddot{q}_r)s \quad (16)$$

$$\dot{\hat{w}}_I = \Lambda_I \text{diag}[q_c - q_r]s \quad (17)$$

where Λ and Λ_I are diagonal positive definite matrices, and Γ_k and Γ_d are symmetric positive definite matrices.

Theorem 1: Suppose that \hat{K}_I is uniformly positive definite and $\hat{J}(q)$ has full row rank. Then, the adaptive outer loop controller given by

(11), (12), (14), (15), (16), and (17) for the robotic system (2) and (3) under the inner PI controller (6) ensures the stability of the system and convergence of the task-space position error, i.e., $\Delta x \rightarrow 0$ as $t \rightarrow \infty$.

Proof: Substituting (6) and (11) into the manipulator dynamics (3) and taking into account Property 4 gives

$$\begin{aligned}
M(q)\dot{s} + C(q, \dot{q})s &= -Bs - K^*(\dot{q} + \mathcal{K}_I q) + K^* \left(\dot{q}_c + \hat{\mathcal{K}}_I q_c \right) \\
&\quad - K^* \Delta \mathcal{K}_I q_c - Y_d(q, \dot{q}, \ddot{q}_r, \ddot{q}_r) a_d \\
&= -Bs - K^*(\dot{q} + \mathcal{K}_I q) + K^* \left(\dot{q}_r + \hat{\mathcal{K}}_I q_r \right) \\
&\quad + K^* \text{diag}[\hat{w}_i, i = 1, \dots, n] \left[-\alpha \hat{J}^T(q) \Delta x + Y_d(q, \dot{q}, \ddot{q}_r, \ddot{q}_r) \hat{a}_d \right] \\
&\quad - K^* \Delta \mathcal{K}_I q_c - Y_d(q, \dot{q}, \ddot{q}_r, \ddot{q}_r) a_d \\
&= -Bs - K^*(\dot{q} + \mathcal{K}_I q) + K^* (\dot{q}_r + \mathcal{K}_I q_r) \\
&\quad + K^* \text{diag}[\hat{w}_i, i = 1, \dots, n] \left[-\alpha \hat{J}^T(q) \Delta x + Y_d(q, \dot{q}, \ddot{q}_r, \ddot{q}_r) \hat{a}_d \right] \\
&\quad - K^* \Delta \mathcal{K}_I (q_c - q_r) - Y_d(q, \dot{q}, \ddot{q}_r, \ddot{q}_r) a_d \\
&= -(K^* + B)s - K \mathcal{K}_I \left[q - q(0) - \int_0^t \dot{q}_r(\sigma) d\sigma + \delta_0 \right] \\
&\quad + K^* \text{diag}[\hat{w}_i, i = 1, \dots, n] \left[-\alpha \hat{J}^T(q) \Delta x + Y_d(q, \dot{q}, \ddot{q}_r, \ddot{q}_r) \hat{a}_d \right] \\
&\quad - Y_d(q, \dot{q}, \ddot{q}_r, \ddot{q}_r) a_d \\
&= -(K^* + B)s - \alpha \hat{J}^T(q) \Delta x - K \mathcal{K}_I \left[\int_0^t s(\sigma) d\sigma + \delta_0 \right] \\
&\quad + K^* (\text{diag}[\hat{w}_i - k_i^{*-1}, i = 1, \dots, n]) \\
&\quad \times [-\alpha \hat{J}^T(q) \Delta x + Y_d(q, \dot{q}, \ddot{q}_r, \ddot{q}_r) \hat{a}_d] \\
&\quad - K^* \Delta \mathcal{K}_I (q_c - q_r) + Y_d(q, \dot{q}, \ddot{q}_r, \ddot{q}_r) \Delta a_d \\
&= -(K^* + B)s - \alpha \hat{J}^T(q) \Delta x - K \mathcal{K}_I \left[\int_0^t s(\sigma) d\sigma + \delta_0 \right] \\
&\quad + \text{diag}[-\alpha \hat{J}^T(q) \Delta x + Y_d(q, \dot{q}, \ddot{q}_r, \ddot{q}_r) \hat{a}_d] K^* \Delta w \\
&\quad - K^* \text{diag}[q_c - q_r] \Delta w_I + Y_d(q, \dot{q}, \ddot{q}_r, \ddot{q}_r) \Delta a_d \quad (18)
\end{aligned}$$

where $\delta_0 = q(0) - q_r(0)$ is a constant vector, $K^* = K K_P = \text{diag}[k_{ii}^*, i = 1, \dots, n]$ with $k_{ii}^*, i = 1, \dots, n$ being positive constants, $\Delta a_d = \hat{a}_d - a_d$, $\Delta w = [\hat{w}_1 - k_{11}^{*-1}, \dots, \hat{w}_n - k_{nn}^{*-1}]^T$, and $\Delta w_I = \hat{w}_I - w_I$ with the entries of w_I being from the diagonal entries of \mathcal{K}_I . Consider the following Lyapunov function candidate

$$\begin{aligned}
V &= \alpha \left(\frac{1}{2} \Delta x^T \Delta x + \frac{1}{2} y^T K_2 K_1^{-1} y + \frac{1}{2} \Delta a_k^T \Gamma_k^{-1} \Delta a_k \right) \\
&\quad + \frac{1}{2} s^T M(q) s + \frac{1}{2} \left[\int_0^t s(\sigma) d\sigma + \delta_0 \right]^T K \mathcal{K}_I \left[\int_0^t s(\sigma) d\sigma + \delta_0 \right] \\
&\quad + \frac{1}{2} \Delta w^T \Lambda^{-1} K^* \Delta w + \frac{1}{2} \Delta a_d^T \Gamma_d^{-1} \Delta a_d + \frac{1}{2} \Delta w_I^T \Lambda_I^{-1} K^* \Delta w_I \quad (19)
\end{aligned}$$

whose derivative with respect to time along the trajectories of (18), (7), (10), (14), (15), (16), and (17) can be written as (using Property 3)

$$\dot{V} = -\alpha y^T K_2 y - s^T (K^* + B) s \leq 0. \quad (20)$$

Then we obtain that $y \in \mathcal{L}_2 \cap \mathcal{L}_\infty$, $s \in \mathcal{L}_2 \cap \mathcal{L}_\infty$, $\int_0^t s(\sigma) d\sigma \in \mathcal{L}_\infty$, $\Delta x \in \mathcal{L}_\infty$, $\hat{w} \in \mathcal{L}_\infty$, $\hat{a}_k \in \mathcal{L}_\infty$, $\hat{a}_d \in \mathcal{L}_\infty$, and $\hat{w}_I \in \mathcal{L}_\infty$. From (7), we obtain that $\dot{y} \in \mathcal{L}_\infty$ and thus y is uniformly continuous. From the properties of square-integrable and uniformly continuous functions [36, p. 232], we obtain that $y \rightarrow 0$ as $t \rightarrow \infty$. From (8), we know that $\dot{q}_r \in \mathcal{L}_\infty$ and thus $\dot{q} \in \mathcal{L}_\infty$. From (14), we obtain that $\hat{a}_k \in \mathcal{L}_\infty$, giving rise to the boundedness of $\hat{J}(q)$. From (2), we obtain that $\dot{x} \in \mathcal{L}_\infty$, and we then obtain that $\dot{y} \in \mathcal{L}_\infty$ based on (7). This means that \dot{y} is uniformly continuous and thus $\dot{y} \rightarrow 0$ as $t \rightarrow \infty$ according to Barbalat's Lemma [35]. From (7), we then obtain that

$\hat{J}^T(q) \Delta x \rightarrow 0$ as $t \rightarrow \infty$. This means that $\Delta x \rightarrow 0$ as $t \rightarrow \infty$ since $\hat{J}(q)$ has full row rank. Furthermore, the result that $\dot{y} \in \mathcal{L}_\infty$ yields the conclusion that $\ddot{q}_r \in \mathcal{L}_\infty$. Rewrite (11) as

$$\begin{aligned}
&(\dot{q}_c - \dot{q}_r) + \hat{\mathcal{K}}_I (q_c - q_r) \\
&= \text{diag}[\hat{w}_i, i = 1, \dots, n] \left[-\alpha \hat{J}^T(q) \Delta x + Y_d(q, \dot{q}, \ddot{q}_r, \ddot{q}_r) \hat{a}_d \right],
\end{aligned}$$

and it can be directly shown that $q_c - q_r \in \mathcal{L}_\infty$ and $\dot{q}_c - \dot{q}_r \in \mathcal{L}_\infty$ since $\hat{\mathcal{K}}_I$ is uniformly positive definite. We then obtain that $\dot{q}_c \in \mathcal{L}_\infty$. From (18), we obtain that $\dot{s} \in \mathcal{L}_\infty$ using Property 2, and further that $\dot{q} \in \mathcal{L}_\infty$. Hence s is uniformly continuous, yielding the result that $s \rightarrow 0$ as $t \rightarrow \infty$ according to the properties of square-integrable and uniformly continuous functions [36, p. 232]. This immediately gives the conclusion that $\dot{q} \rightarrow 0$ as $t \rightarrow \infty$ since $\dot{q}_r = -K_2 y \rightarrow 0$ as $t \rightarrow \infty$. ■

Remark 1: The introduction of the adaptive scales \hat{w} and \hat{w}_I is to accommodate the uncertain diagonal matrices $K^* = K K_P$ and $K_P^{-1} K_I$, and their uncertainty comes from both the actuator model and low-level controller design (generally performed by the robot production company). The part due to the actuator model (i.e., K) is inherently uncertain and may possibly be subjected to slow variation. The uncertainty of the part due to the low-level controller design (i.e., K_P and K_I) is a business strategy for protecting the intellectual property right and thus it is and will be impossible to be disclosed thoroughly in the short run. In addition, the adaptive scale \hat{w} used here is computationally efficient and free of computational singularity since it does not involve the computation of inverse of an estimated quantity (which, however, would be encountered if we directly estimate the matrix K^*). Similar techniques for handling the uncertainty of the diagonal torque-constant matrix (which describes the relation between the torque and current) appear in the context of adaptive control for rigid-link electrically-driven robots or robots with actuator uncertainty, yet with an open controller structure (i.e., the voltage can be directly specified by the user) [37], [11].

Remark 2: The uniform positive definiteness of $\hat{\mathcal{K}}_P$ can be conveniently ensured by using the projection algorithms [38], and the full row rank of $\hat{J}(q)$ can be ensured by the assumption of being away from the singular configuration and the use of the projection algorithms [21], [13].

Remark 3: The adaptive filter (7) with $K_1 \hat{J}^T(q) \Delta x$ as the input can be considered as an extension of [39] to address the avoidance of task-space velocity measurement in the context of adaptive task-space control. Clearly, the joint velocity command given by (11) no longer involves the task-space velocity measurement since $\ddot{q}_r = -K_2 \dot{y}$ and \dot{y} given by (7) does not involve the task-space velocity.

B. Observer-Based Adaptive Regulation Control

The task-space observer is given as

$$\dot{x}_o = \hat{J}(q) \dot{q}_r - \beta \hat{J}(q) \hat{J}^T(q) \Delta x_o \quad (21)$$

where $x_o \in R^m$ denotes the observed quantity of x , $\Delta x_o = x_o - x$, and β is a positive design constant, and the joint reference velocity \dot{q}_r is now defined as

$$\dot{q}_r = -\hat{J}^T(q) [\gamma(x_o - x_d)] \quad (22)$$

where γ is a positive design constant. The observer (21) is motivated by [26] yet with a new feedback gain $\beta \hat{J}(q) \hat{J}^T(q)$ for the purpose of achieving feedback separation, and the idea behind is that the actual joint velocity finally approaches the joint reference velocity \dot{q}_r and thus $\hat{J}(q) \dot{q}_r$ would approach the estimated task-space velocity $\hat{J}(q) \dot{q}$. The desirable point is that the observer no longer depends on the joint

velocity and is thus not influenced by the noise of the velocity signal. The joint velocity command is defined as

$$\dot{q}_c + \hat{K}_I q_c = \dot{q}_r + \hat{K}_I q_r + \text{diag}[\hat{w}_i, i = 1, \dots, n] \times Y_d(q, \dot{q}, \ddot{q}_r) \hat{a}_d \quad (23)$$

which no longer needs the scaled dynamic compensation action $\text{diag}[\hat{w}_i, i = 1, \dots, n] [-\alpha \hat{J}^T(q) \Delta x]$. The adaptation laws for \hat{a}_k and \hat{w} are given as

$$\dot{\hat{a}}_k = \Gamma_k Y_k^T(q, \dot{q})(\Delta x - \Delta x_o) \quad (24)$$

$$\dot{\hat{w}} = -\Lambda \text{diag}[Y_d(q, \dot{q}, \ddot{q}_r) \hat{a}_d] s \quad (25)$$

The adaptation laws for \hat{a}_d and \hat{w}_I remain the same as (16) and (17), respectively.

Combining (21) and (2) and using Property 1 yields

$$\Delta \dot{x}_o = -\beta \hat{J}(q) \hat{J}^T(q) \Delta x_o + Y_k(q, \dot{q}) \Delta a_k - \hat{J}(q) s. \quad (26)$$

By premultiplying $s = \dot{q} - \dot{q}_r$ with $\hat{J}(q)$ and using Property 1, we obtain

$$\hat{J}(q) s = \dot{x} + \hat{J}(q) \hat{J}^T(q) [\gamma(x_o - x_d)] + Y_k(q, \dot{q}) \Delta a_k. \quad (27)$$

Therefore, at the outer loop, we obtain

$$\Delta \dot{x}_o = -\beta \hat{J}(q) \hat{J}^T(q) \Delta x_o + Y_k(q, \dot{q}) \Delta a_k - \hat{J}(q) s \quad (28)$$

$$\dot{x} = -\hat{J}(q) \hat{J}^T(q) [\gamma(x_o - x_d)] - Y_k(q, \dot{q}) \Delta a_k + \hat{J}(q) s. \quad (29)$$

We are presently ready to formulate the following theorem.

Theorem 2: Suppose that \hat{K}_I is uniformly positive definite and $\hat{J}(q)$ has full row rank, and let the controller parameters β and γ be chosen such that

$$\beta > 4\gamma/9. \quad (30)$$

The adaptive outer loop controller given by (23), (12), (21), (24), (25), (16), and (17) with \dot{q}_r being given as (22) for the robotic system (2) and (3) under the inner PI controller (6) ensures the stability of the system and convergence of the task-space position error, i.e., $\Delta x \rightarrow 0$ as $t \rightarrow \infty$.

Proof: Substituting (6), (23), and (12) into (3) and using Property 4 gives

$$\begin{aligned} M(q) \dot{s} + C(q, \dot{q}) s = & -(K^* + B) s - K K_I \left[\int_0^t s(\sigma) d\sigma + \delta_0 \right] \\ & + \text{diag}[Y_d(q, \dot{q}, \ddot{q}_r) \hat{a}_d] K^* \Delta w \\ & - K^* \text{diag}[q_c - q_r] \Delta w_I \\ & + Y_d(q, \dot{q}, \ddot{q}_r) \Delta a_d. \end{aligned} \quad (31)$$

Consider the Lyapunov-like function candidate

$$\begin{aligned} V^* = & \frac{1}{2} s^T M(q) s + \frac{1}{2} \left[\int_0^t s(\sigma) d\sigma + \delta_0 \right]^T K K_I \\ & \times \left[\int_0^t s(\sigma) d\sigma + \delta_0 \right] + \frac{1}{2} \Delta w^T \Lambda^{-1} K^* \Delta w \\ & + \frac{1}{2} \Delta a_d^T \Gamma_d^{-1} \Delta a_d + \frac{1}{2} \Delta w_I^T \Lambda_I^{-1} K^* \Delta w_I \end{aligned} \quad (32)$$

whose derivative with respect to time along the trajectories of (31), (25), (16), and (17) can be written as

$$\dot{V}^* = -s^T (K^* + B) s \leq 0 \quad (33)$$

where we have used Property 3. This directly gives the conclusion that $s \in \mathcal{L}_2 \cap \mathcal{L}_\infty$, $\int_0^t s(r) dr \in \mathcal{L}_\infty$, $\hat{w} \in \mathcal{L}_\infty$, $\hat{a}_d \in \mathcal{L}_\infty$, and $\hat{w}_I \in \mathcal{L}_\infty$. Then, there exists a positive constant ℓ_M such that

$\int_0^t s^T(\sigma) s(\sigma) d\sigma \leq \ell_M$, $\forall t \geq 0$. Let us now consider the following quasi-Lyapunov function candidate

$$\begin{aligned} V^{**} = & \frac{1}{2} \Delta x_o^T \Delta x_o + \frac{1}{2} \Delta x^T \Delta x + \frac{1}{2} \Delta a_k^T \Gamma_k^{-1} \Delta a_k \\ & + \left(\frac{1}{\beta} + \frac{1}{\gamma} \right) \left[\ell_M - \int_0^t s^T(\sigma) s(\sigma) d\sigma \right] \end{aligned} \quad (34)$$

with the choice of the last term following the typical practice (see, e.g., [40, p. 118]), and the derivative of V^{**} along the trajectories of (28), (29), and (24) can be written as

$$\begin{aligned} \dot{V}^{**} = & -\beta \Delta x_o^T \hat{J}(q) \hat{J}^T(q) \Delta x_o \\ & - \Delta x_o^T \hat{J}(q) s - \gamma \Delta x^T \hat{J}(q) \hat{J}^T(q) \Delta x_o \\ & - \gamma \Delta x^T \hat{J}(q) \hat{J}^T(q) \Delta x + \Delta x^T \hat{J}(q) s - \left(\frac{1}{\beta} + \frac{1}{\gamma} \right) s^T s. \end{aligned} \quad (35)$$

Using the following results derived from the standard basic inequalities

$$\Delta x_o^T \hat{J}(q) s \leq \frac{\beta}{4} \Delta x_o^T \hat{J}(q) \hat{J}^T(q) \Delta x_o + \frac{1}{\beta} s^T s \quad (36)$$

$$\Delta x^T \hat{J}(q) s \leq \frac{\gamma}{4} \Delta x^T \hat{J}(q) \hat{J}^T(q) \Delta x + \frac{1}{\gamma} s^T s \quad (37)$$

we obtain from (35) that

$$\begin{aligned} \dot{V}^{**} \leq & -\frac{3\beta}{4} \Delta x_o^T \hat{J}(q) \hat{J}^T(q) \Delta x_o \\ & - \gamma \Delta x^T \hat{J}(q) \hat{J}^T(q) \Delta x_o - \frac{3\gamma}{4} \Delta x^T \hat{J}(q) \hat{J}^T(q) \Delta x \\ \leq & - \underbrace{\begin{bmatrix} \hat{J}^T(q) \Delta x_o \\ \hat{J}^T(q) \Delta x \end{bmatrix}^T \begin{bmatrix} (3\beta/4) I_n & (\gamma/2) I_n \\ (\gamma/2) I_n & (3\gamma/4) I_n \end{bmatrix} \begin{bmatrix} \hat{J}^T(q) \Delta x_o \\ \hat{J}^T(q) \Delta x \end{bmatrix}}_Q \leq 0 \end{aligned} \quad (38)$$

due to the positive definiteness of Q in the case that $\beta > 4\gamma/9$, where I_n is the $n \times n$ identity matrix. Then using similar procedures as in the proof of Theorem 1, we can show the stability of the system [regardless of the estimated Jacobian matrix $\hat{J}(q)$] and the convergence of Δx and Δx_o . ■

Remark 4: The existing adaptive (or robust) task-space regulation algorithms either assume the exact knowledge of the gravitational torques [21], [12], or require the careful choice of the controller parameters [20], [41], [22], or encounter the overparametrization problem [22]. Furthermore, many adaptive visual tracking schemes (e.g., [21], [24], [14], [25]) have also been proposed, yet the necessity of investigating task-space regulation algorithms is due to the consideration that the choice of specific controllers should take into account the properties of the specific tasks. It is well accepted that given a specific task, the control law should be as (computationally) simple as possible; while the adaptive tracking controllers can also achieve the regulation of the task-space position to the desired one (constant), it is not cost-effective to rely on such kind of complexity (usually involves the inverse of the estimated Jacobian and the singularity issues) for regulation tasks. The two adaptive regulation controllers presented here rule out the limitations of the above results, and in addition the proposed controllers can be applied to robotic systems with an inner/outer loop structure (e.g., most industrial/commercial robotic systems) that have an unmodifiable joint servoing controller but admit the design of the joint velocity (or position) command, benefiting from the dynamic feedback design and the use of the adaptively scaled dynamic compensation action.

C. Extension to Task-Space Tracking

In the case of task-space tracking, a feedforward action needs to be introduced in the definition of the joint reference velocity. Specifically we define \dot{q}_r as

$$\dot{q}_r = \underbrace{\hat{J}^T(q)[\hat{J}(q)\hat{J}^T(q)]^{-1}\dot{x}_d}_{\text{feedforward}} - \underbrace{\gamma\hat{J}^T(q)(x_o - x_d)}_{\text{feedback}} \quad (39)$$

where the use of the generalized inverse of $\hat{J}(q)$ follows the typical practice. The definition given by (39) extends the one in [30] to address the case of no task-space velocity measurement. The interesting point here is that both the inverse and transpose of $\hat{J}(q)$ are incorporated, and one is for introducing a feedforward action and the other for introducing a feedback action. This is in contrast to most existing task-space control algorithms that rely on the use of the inverse of the (estimated) Jacobian matrix to exert both the feedforward and feedback actions (see, e.g., [9], [32], [14]). As can be clearly observed, once the desired task-space velocity becomes zero, \dot{q}_r in (39) reduces to the one defined by (22), and this means that the regulation and tracking cases are unified.

Theorem 3: Suppose that \hat{K}_I is uniformly positive definite and $\hat{J}(q)$ has full row rank, and let the controller parameters β and γ be chosen such that

$$\beta > 4\gamma/9. \quad (40)$$

The adaptive outer loop controller given by (23), (12), (21), (24), (25), (16), and (17) with \dot{q}_r being given as (39) for the robotic system (2) and (3) under the inner PI controller (6) ensures the stability of the system and convergence of the task-space tracking errors, i.e., $\Delta x \rightarrow 0$ and $\Delta \dot{x} \rightarrow 0$ as $t \rightarrow \infty$.

The proof of Theorem 3 can be straightforwardly completed based on that of Theorem 2, and the major difference lies in the fact that equation (29) for the case of regulation problem now becomes

$$\Delta \dot{x} = -\hat{J}(q)\hat{J}^T(q)[\gamma(x_o - x_d)] - Y_k(q, \dot{q})\Delta a_k + \hat{J}(q)s. \quad (41)$$

By an analysis of the system given by (28), (41), and (24), we can derive the stability of the system and convergence of the task-space tracking errors.

Remark 5: The filter-based adaptive regulation algorithm is computationally simpler in comparison with the observer-based one. But the main issue of the filter-based algorithm is that it is difficult to quantitatively evaluate the performance. Here the observer-based algorithm is extended to cover the case of task-space tracking by additionally introducing feedforward based on the generalized inverse of the estimated Jacobian matrix [see (39)]. The extension of the filter-based algorithm to realize the task-space tracking can be completed in a similar way.

D. Task-Space Adaptive Control With an Inner PID Position Controller

We here investigate another case that the low-level controller takes the PID position control action, i.e.,

$$u = -K_D(\dot{q} - \dot{q}_c) - K_P(q - q_c) - K_I \int_0^t [q(\sigma) - q_c(\sigma)]d\sigma \quad (42)$$

where K_D , K_P , and K_I are the derivative, proportional, and integral gains (diagonal and positive definite), respectively. In this case, to ensure the stability and convergence of the robotic system, we need to make some modifications. We take the filter-based adaptive regulation control in Sec. III-A as an illustrating example and the other controllers can be similarly formulated. Specifically, we define

two quantities below

$$\dot{q}_r^* = \dot{q}_r - K_c(q - q_r) \quad (43)$$

$$\ddot{q}_r^* = \ddot{q}_r - K_c(\dot{q} - \dot{q}_r) \quad (44)$$

with q_r being generated by

$$\dot{q}_r = -K_c q_r - K_2 y + K_c q \quad (45)$$

where K_c is a diagonal positive definite matrix. Let $\mathcal{K}_P = K_D^{-1}K_P$ and $\mathcal{K}_I = K_D^{-1}K_I$ and denote by $\hat{\mathcal{K}}_P$ and $\hat{\mathcal{K}}_I$ the estimate of \mathcal{K}_P and that of \mathcal{K}_I , respectively, which are specifically written as

$$\hat{\mathcal{K}}_P = \text{diag}[\hat{w}_P] \quad (46)$$

$$\hat{\mathcal{K}}_I = \text{diag}[\hat{w}_I] \quad (47)$$

with \hat{w}_P and \hat{w}_I being n -dimensional vectors. The joint velocity command for the low-level PID controller is defined as

$$\begin{aligned} \dot{q}_c + \hat{\mathcal{K}}_P q_c + \hat{\mathcal{K}}_I \int_0^t [q_c(\sigma) - q_r(\sigma)]d\sigma \\ = \dot{q}_r^* + \hat{\mathcal{K}}_P q_r + \text{diag}[\hat{w}_i, i = 1, \dots, n] \\ \times [-\alpha \hat{J}^T(q)\Delta x + Y_d(q, \dot{q}, \dot{q}_r^*, \ddot{q}_r^*)\hat{a}_d]. \end{aligned} \quad (48)$$

The adaptation laws for \hat{w} , \hat{a}_d , \hat{w}_P , and \hat{w}_I are now given as

$$\dot{\hat{w}} = -\Lambda \text{diag}[-\alpha \hat{J}^T(q)\Delta x + Y_d(q, \dot{q}, \dot{q}_r^*, \ddot{q}_r^*)\hat{a}_d]\xi \quad (49)$$

$$\dot{\hat{a}}_d = -\Gamma_d Y_d^T(q, \dot{q}, \dot{q}_r^*, \ddot{q}_r^*)\xi \quad (50)$$

$$\dot{\hat{w}}_P = \Lambda_P \text{diag}[q_c - q_r]\xi \quad (51)$$

$$\dot{\hat{w}}_I = \Lambda_I \text{diag}\left[\int_0^t [q_c(\sigma) - q_r(\sigma)]d\sigma\right]\xi \quad (52)$$

with

$$\xi = \dot{q} - \dot{q}_r^* = s + K_c \left[\int_0^t s(\sigma)d\sigma + \delta_0 \right], \quad (53)$$

and Λ_P and Λ_I being diagonal positive definite matrices, and the adaptation law for \hat{a}_k is still the same as (14).

With these modifications and using the fact that $q - q_r =$

$\int_0^t s(\sigma)d\sigma + \delta_0$, equation (18) becomes

$$\begin{aligned}
& M(q)\dot{\xi} + C(q, \dot{q})\xi \\
& = -(\bar{K}^* + B)\xi - \alpha \hat{J}^T(q)\Delta x \\
& \quad - KK_P(q - q_r) - KK_I \int_0^t [q(\sigma) - q_r(\sigma)]d\sigma \\
& \quad + \text{diag}[-\alpha \hat{J}^T(q)\Delta x + Y_d(q, \dot{q}, \ddot{q}_r^*, \ddot{q}_r^*)\hat{a}_d]\bar{K}^*\Delta w \\
& \quad - \bar{K}^*\text{diag}[q_c - q_r]\Delta w_P - \bar{K}^*\text{diag}\left[\int_0^t [q_c(\sigma) - q_r(\sigma)]d\sigma\right]\Delta w_I \\
& \quad + Y_d(q, \dot{q}, \ddot{q}_r^*, \ddot{q}_r^*)\Delta a_d \\
& = -(\bar{K}^* + B)\xi - \alpha \hat{J}^T(q)\Delta x - (KK_P - KK_I K_c^{-1})(q - q_r) \\
& \quad - KK_I K_c^{-1}\left[q - q_r + K_c \int_0^t [q(\sigma) - q_r(\sigma)]d\sigma\right] \\
& \quad + \text{diag}[-\alpha \hat{J}^T(q)\Delta x + Y_d(q, \dot{q}, \ddot{q}_r^*, \ddot{q}_r^*)\hat{a}_d]\bar{K}^*\Delta w \\
& \quad - \bar{K}^*\text{diag}[q_c - q_r]\Delta w_P - \bar{K}^*\text{diag}\left[\int_0^t [q_c(\sigma) - q_r(\sigma)]d\sigma\right]\Delta w_I \\
& \quad + Y_d(q, \dot{q}, \ddot{q}_r^*, \ddot{q}_r^*)\Delta a_d \\
& = -(\bar{K}^* + B)\xi - \alpha \hat{J}^T(q)\Delta x \\
& \quad - (KK_P - KK_I K_c^{-1})\left[\int_0^t s(\sigma)d\sigma + \delta_0\right] \\
& \quad - KK_I K_c^{-1}\left[\int_0^t \xi(\sigma)d\sigma + \delta_0\right] \\
& \quad + \text{diag}[-\alpha \hat{J}^T(q)\Delta x + Y_d(q, \dot{q}, \ddot{q}_r^*, \ddot{q}_r^*)\hat{a}_d]\bar{K}^*\Delta w \\
& \quad - \bar{K}^*\text{diag}[q_c - q_r]\Delta w_P - \bar{K}^*\text{diag}\left[\int_0^t [q_c(\sigma) - q_r(\sigma)]d\sigma\right]\Delta w_I \\
& \quad + Y_d(q, \dot{q}, \ddot{q}_r^*, \ddot{q}_r^*)\Delta a_d \tag{54}
\end{aligned}$$

where $\bar{K}^* = KK_D$. The above equation can further be written as

$$\begin{aligned}
& M(q)\dot{\xi} + C(q, \dot{q})\xi \\
& = \text{diag}[-\alpha \hat{J}^T(q)\Delta x + Y_d(q, \dot{q}, \ddot{q}_r^*, \ddot{q}_r^*)\hat{a}_d]\bar{K}^*\Delta w \\
& \quad - \bar{K}^*\text{diag}[q_c - q_r]\Delta w_P - \bar{K}^*\text{diag}\left[\int_0^t [q_c(\sigma) - q_r(\sigma)]d\sigma\right]\Delta w_I \\
& \quad + Y_d(q, \dot{q}, \ddot{q}_r^*, \ddot{q}_r^*)\Delta a_d - \alpha \hat{J}^T(q)\Delta x \\
& \quad - K[(K_D + K^{-1}B)s \\
& \quad + ((K_D + K^{-1}B)K_c + (K_P - K_I K_c^{-1}))\left(\int_0^t s(\sigma)d\sigma + \delta_0\right)] \\
& \quad - KK_I K_c^{-1}\left[\int_0^t \xi(\sigma)d\sigma + \delta_0\right]. \tag{55}
\end{aligned}$$

Consider the Lyapunov function candidate

$$\begin{aligned}
V = & \alpha\left(\frac{1}{2}\Delta x^T \Delta x + \frac{1}{2}y^T K_2 K_1^{-1}y + \frac{1}{2}\Delta a_k^T \Gamma_k^{-1}\Delta a_k\right) \\
& + \frac{1}{2}\xi^T M(q)\xi + \frac{1}{2}\left[\int_0^t \xi(\sigma)d\sigma + \delta_0\right]^T KK_I \left[\int_0^t \xi(\sigma)d\sigma + \delta_0\right] \\
& + \frac{1}{2}\left[\int_0^t s(\sigma)d\sigma + \delta_0\right]^T (KM + KK_c K_D + K_c B) \\
& \times \left[\int_0^t s(\sigma)d\sigma + \delta_0\right] + \frac{1}{2}\Delta w^T \Lambda^{-1}\bar{K}^*\Delta w + \frac{1}{2}\Delta a_d^T \Gamma_d^{-1}\Delta a_d \\
& + \frac{1}{2}\Delta w_P^T \Lambda_P^{-1}\bar{K}^*\Delta w_P + \frac{1}{2}\Delta w_I^T \Lambda_I^{-1}\bar{K}^*\Delta w_I \tag{56}
\end{aligned}$$

where

$$\mathcal{M} = (K_D + K^{-1}B)K_c + K_P - K_I K_c^{-1}. \tag{57}$$

By suitably choosing K_c , we can ensure that \mathcal{M} is positive semidef-

inite. The derivative of V can be written as

$$\begin{aligned}
\dot{V} = & -\alpha y^T K_2 y - s^T (\bar{K}^* + B)s \\
& - \left[\int_0^t s(\sigma)d\sigma + \delta_0\right]^T K \mathcal{M} K_c \left[\int_0^t s(\sigma)d\sigma + \delta_0\right] \leq 0. \tag{58}
\end{aligned}$$

Theorem 4: Suppose that \hat{K}_P and \hat{K}_I evolve such that the following system

$$\ddot{z} + \hat{K}_P \dot{z} + \hat{K}_I z = 0 \tag{59}$$

with $z \in R^n$ is uniformly exponentially stable and that $\hat{J}(q)$ has full row rank, and choose the matrix K_c such that \mathcal{M} given by (57) is positive semidefinite. Then the adaptive outer loop controller given by (48), (12), (7), (45), (49), (50), (51), (52), and (14) for the robotic system (2) and (3) under the inner PID position controller (42) ensures the stability of the system and convergence of the task-space position error, i.e., $\Delta x \rightarrow 0$ as $t \rightarrow \infty$.

The proof of Theorem 4 can be completed by following similar steps as in the proof of Theorem 1.

Remark 6:

- 1) One key issue in the case of using a low-level PID controller is the choice of K_c , and obviously large enough K_c can ensure that \mathcal{M} is positive semidefinite. The remaining thing is how to determine the gain K_c . In practice, since the damping matrix B may be quite small, we thus neglect it and this implies that $k_{c,ii}$ (i.e., the i -th diagonal entry of K_c) should satisfy

$$k_{c,ii} \geq \frac{2k_{I,ii}}{k_{P,ii} + \sqrt{k_{P,ii}^2 + 4k_{I,ii}k_{D,ii}}}, \forall i = 1, \dots, n \tag{60}$$

where $k_{D,ii}$ is the i -th diagonal entry of K_D , $k_{P,ii}$ is the i -th diagonal entry of K_P , and $k_{I,ii}$ is the i -th diagonal entry of K_I . Here we face the similar situation as the control engineers of the robot production company. The control engineers are usually careful about the choice of the integral gain and large gain may cause instability; a trade-off has to be made between the attenuation of constant disturbances and the stability margin of the control system. In practice, $k_{P,ii}$ and $k_{D,ii}$ are possibly/generally chosen to be not less than $k_{I,ii}$, and in this case, we can simply choose $k_{c,ii}$ as $k_{c,ii} \geq (\sqrt{5} - 1)/2$, $\forall i = 1, \dots, n$.

- 2) An important issue in proving Theorem 4 is to clarify the input-output properties of the following system [derived from (48)]

$$\begin{aligned}
& \dot{q}_c - \dot{q}_r + \hat{K}_P(q_c - q_r) + \hat{K}_I \int_0^t [q_c(\sigma) - q_r(\sigma)]d\sigma \\
& = \text{diag}[\hat{w}_i, i = 1, \dots, n] \left[-\alpha \hat{J}^T(q)\Delta x + Y_d(q, \dot{q}, \ddot{q}_r^*, \ddot{q}_r^*)\hat{a}_d \right] \\
& \quad - K_c(q - q_r) \tag{61}
\end{aligned}$$

where the right side is bounded. The main issue can now be reduced to investigating the stability of the linear time-varying system (59). By the assumption that the system (59) is uniformly exponentially stable, we can directly obtain from (61) that $\int_0^t [q_c(\sigma) - q_r(\sigma)]d\sigma$, $q_c - q_r$, and $\dot{q}_c - \dot{q}_r$ are bounded. Then the boundedness of \ddot{q} can be ensured.

On the other hand, by the standard projection algorithms [38], we can conveniently ensure that \hat{K}_P and \hat{K}_I are uniformly positive. In addition, the boundedness of \hat{K}_P and \hat{K}_I is a direct consequence of that of the Lyapunov function candidate given by (56). But even under these two conditions, we still cannot ensure the uniform exponential stability of (59) [which is a sufficient condition to ensure the uniform bounded-input bounded-output stability of (61) according to the standard linear

system theory] since the coefficient matrices are time-varying. In practice, we may slow down the adaptation to \mathcal{K}_P and \mathcal{K}_I (i.e., slow down the variation of $\hat{\mathcal{K}}_P$ and $\hat{\mathcal{K}}_I$) so that the system (59) is a slowly time-varying (or quasi-time-invariant) linear system.

IV. GENERALIZATIONS AND FURTHER DISCUSSIONS

Let us now discuss the proposed framework in other closely related topics concerning adaptive robot control.

A. Direct Adaptation

The first result that we would like to discuss is the well-known Slotine and Li adaptive controller [9] and the result there is presented in the context of open joint torque control. If we redefine \dot{q}_r in (22) as

$$\dot{q}_r = \dot{q}_d - \bar{\alpha}(q - q_d) \quad (62)$$

with $q_d \in R^n$ being the desired joint position and $\bar{\alpha}$ a positive design constant, then the adaptive controller given by (23), (12), (15), (16), and (17) with \dot{q}_r being defined by (62) becomes an outer loop (“applicable”) version of Slotine and Li adaptive controller suitable for practical robotic systems (without opening the torque control module) with an unmodifiable inner PI velocity control loop (in the case of an inner PID position controller, its outer loop version can be similarly developed by following the steps in Sec. III-D). In this case of the joint-space position tracking, one can easily show that the position command $q_c = q_d$ is also qualified for ensuring the stability of the robotic system and convergence of the joint tracking errors.

B. Composite Adaptation

The implementation of the standard composition adaptation algorithm given in [42] in the framework of inner/outer controller structure seems not straightforward and we need to ensure that no additional number of parameters appear in the filtered dynamic model (i.e., avoiding the overparameterization). For this purpose, we rewrite the dynamics (3) as

$$\begin{aligned} \text{diag}[w_i, i = 1, \dots, n][M(q)\ddot{q} + C(q, \dot{q})\dot{q} + B\dot{q} + g(q)] \\ = K_P^{-1}u = -(\dot{q} - \dot{q}_c) - K_P^{-1}K_I(q - q_c) \end{aligned} \quad (63)$$

and by using the filtering technique in [42], we then have the following equation without involving joint acceleration measurement

$$\begin{aligned} \text{diag}[w_i, i = 1, \dots, n]Y_f(q, \dot{q}, t)a_d \\ = u_f^* - \text{diag}[w_{I,i}, i = 1, \dots, n]h_f \end{aligned} \quad (64)$$

where $w_i = k_i^{*-1}$, $w_{I,i} = k_{P,ii}^{-1}k_{I,ii}$, $i = 1, \dots, n$, $Y_f(q, \dot{q}, t) = \frac{\lambda_f}{p+\lambda_f}Y_d(q, \dot{q}, \ddot{q})$, $u_f^* = -\frac{\lambda_f}{p+\lambda_f}(\dot{q} - \dot{q}_c)$, and $h_f = \frac{\lambda_f}{p+\lambda_f}(q - q_c)$ with p and $\lambda_f > 0$ being the Laplace variable and the filter parameter, respectively. Let

$$\hat{u}_f^* = \text{diag}[\hat{w}]Y_f\hat{a}_d + \text{diag}[h_f]\hat{w}_I \quad (65)$$

where \hat{w}_I is the estimate of $w_I = [w_{I,1}, \dots, w_{I,n}]^T$. Then we define a prediction error

$$\begin{aligned} e_f = \hat{u}_f^* - u_f^* \\ = \text{diag}[w]Y_f\Delta a_d + \text{diag}[Y_f\hat{a}_d]\Delta w + \text{diag}[h_f]\Delta w_I \end{aligned} \quad (66)$$

and the composite adaptive version of (15), (16), and (17) is given as

$$\dot{\hat{w}} = -\Lambda(\text{diag}[Y_d(q, \dot{q}, \ddot{q})\hat{a}_d]s + \gamma_0\text{diag}[Y_f\hat{a}_d]e_f) \quad (67)$$

$$\dot{\hat{a}}_d = -\Gamma_d(Y_d^T(q, \dot{q}, \ddot{q})s + \gamma_0Y_f^T e_f) \quad (68)$$

$$\dot{\hat{w}}_I = \Lambda_I(\text{diag}[q_c - q_r]s - \gamma_0\text{diag}[h_f]e_f) \quad (69)$$

where γ_0 is a positive design constant.

Remark 7: The interesting and also distinguished point here is that the prediction error e_f given by (66) contains the unknown coefficient matrix $\text{diag}[w]$, due to which the regressor matrix is actually only partially known. This motivates us to wonder whether or not the stability of the closed-loop robotic system can still be guaranteed under the composite adaptation here.

Consider the nonnegative function

$$V_1 = (1/2)[\Delta w^T \Lambda^{-1} K^* \Delta w + \Delta a_d^T \Gamma_d^{-1} \Delta a_d + \Delta w_I^T \Lambda_I^{-1} K^* \Delta w_I] \quad (70)$$

whose derivative along (67), (68), and (69) can be written as

$$\begin{aligned} \dot{V}_1 = & -\Delta w^T K^* \text{diag}[Y_d(q, \dot{q}, \ddot{q})\hat{a}_d]s - \Delta a_d^T Y_d^T(q, \dot{q}, \ddot{q})s \\ & + \Delta w_I^T K^* \text{diag}[q_c - q_r]s - \gamma_0(\Delta w^T K^* \text{diag}[Y_f\hat{a}_d]e_f \\ & + \Delta a_d^T Y_f^T e_f + \Delta w_I^T K^* \text{diag}[h_f]e_f) \\ = & -\Delta w^T K^* \text{diag}[Y_d(q, \dot{q}, \ddot{q})\hat{a}_d]s - \Delta a_d^T Y_d^T(q, \dot{q}, \ddot{q})s \\ & + \Delta w_I^T K^* \text{diag}[q_c - q_r]s - \gamma_0 e_f^T K^* \\ & \times \underbrace{(\text{diag}[Y_f\hat{a}_d]\Delta w + \text{diag}[w]Y_f\Delta a_d + \text{diag}[h_f]\Delta w_I)}_{e_f} \end{aligned} \quad (71)$$

where the first three terms are used to compensate for the indefinite terms due to the parametric uncertainty, and in this way, the stability is ensured. The key point here is to exploit the independent nature of the joint processors which means that K^* is diagonal. The other versions of composite adaptation, e.g., BGF composite adaptation and CF composite adaptation (see, e.g., [42]) can also be used so that smoother parameter adaptation and better tracking performance can be achieved. Specifically, the CF composite adaptation laws can be given as

$$\begin{cases} \dot{\hat{w}} = -\Lambda(\text{diag}[Y_d(q, \dot{q}, \ddot{q})\hat{a}_d]s + \gamma_0\text{diag}[Y_f\hat{a}_d]e_f) \\ \dot{\hat{a}}_d = -\Gamma_d(Y_d^T(q, \dot{q}, \ddot{q})s + \gamma_0Y_f^T e_f) \\ \dot{\hat{w}}_I = \Lambda_I(\text{diag}[q_c - q_r]s - \gamma_0\text{diag}[h_f]e_f) \\ \dot{\hat{\Lambda}} = \lambda_3(\Lambda_I - \Lambda_I\bar{\Lambda}_I^{-1}\Lambda_I) - \gamma_0\Lambda_I(\text{diag}[h_f])^2\Lambda_I \end{cases} \quad (72)$$

where λ_1 , λ_2 , and λ_3 are strictly positive forgetting factors (time-varying or constant), and $\bar{\Lambda}$, $\bar{\Gamma}_d$, and $\bar{\Lambda}_I$ denote the upper bounds of Λ , Γ_d , and Λ_I , respectively. Note that $\Lambda(0)$ and $\Lambda_I(0)$ are chosen as diagonal positive definite matrices satisfying $0 < \Lambda(0) \leq \bar{\Lambda}$ and $0 < \Lambda_I(0) \leq \bar{\Lambda}_I$, and $\Gamma_d(0)$ can be chosen as a symmetric positive definite matrix satisfying $0 < \Gamma_d(0) \leq \bar{\Gamma}_d$, and in this way, it can be shown that $\Lambda(t)$ and $\Lambda_I(t)$ are always diagonal, $\forall t \geq 0$. The derivative of the nonnegative function V_1 defined by (70) in this case becomes

$$\begin{aligned} \dot{V}_1 = & -\Delta w^T K^* \text{diag}[Y_d(q, \dot{q}, \ddot{q})\hat{a}_d]s - \Delta a_d^T Y_d^T(q, \dot{q}, \ddot{q})s \\ & + \Delta w_I^T K^* \text{diag}[q_c - q_r]s \\ & - \frac{\lambda_1}{2}\Delta w^T (\Lambda^{-1} - \bar{\Lambda}^{-1})K^* \Delta w - \frac{\lambda_2}{2}\Delta a_d^T (\Gamma_d^{-1} - \bar{\Gamma}_d^{-1})\Delta a_d \\ & - \frac{\lambda_3}{2}\Delta w_I^T (\Lambda_I^{-1} - \bar{\Lambda}_I^{-1})K^* \Delta w_I - \frac{\gamma_0}{2}e_f^T K^* e_f. \end{aligned} \quad (73)$$

Obviously, the stability of the system and convergence of the joint tracking errors can be guaranteed.

C. Adaptive Control of Flexible-Joint Manipulators

The typical result may be the singular-perturbation-based adaptive control approach [10], [43]. Consider a flexible-joint manipulator

governed by [44]

$$\begin{cases} M_0(q)\ddot{q} + C(q, \dot{q})\dot{q} + B\dot{q} + g(q) = K_s(\theta - q) \\ D_r\ddot{\theta} + B_r\dot{\theta} = Ku - K_s(\theta - q) \end{cases} \quad (74)$$

where $\theta \in R^n$ is the rotor position, K_s is the constant, diagonal, and positive definite stiffness matrix, $D_r \in R^{n \times n}$ is the rotor inertia matrix seen from the link side, and $B_r \in R^{n \times n}$ is the damping matrix. In this case, the motor velocity command is defined as

$$\begin{aligned} \dot{q}_c + \hat{K}_P q_c &= \dot{q}_r + \hat{K}_P q_r + \text{diag}[\hat{w}_i, i = 1, \dots, n] \\ &\times Y_d(q, \dot{q}, \dot{q}_r, \ddot{q}_r) \hat{a}_d \end{aligned} \quad (75)$$

with \dot{q}_r being defined as

$$\dot{q}_r = \dot{q}_d - \bar{\alpha}(q - q_d). \quad (76)$$

The adaptation laws for \hat{w} , \hat{a}_d , and \hat{w}_I are given as

$$\dot{\hat{w}} = -\Lambda \text{diag}[Y_d(q, \dot{q}, \dot{q}_r, \ddot{q}_r) \hat{a}_d] s \quad (77)$$

$$\dot{\hat{a}}_d = -\Gamma_d Y_d^T(q, \dot{q}, \dot{q}_r, \ddot{q}_r) s \quad (78)$$

$$\dot{\hat{w}}_I = \Lambda_I \text{diag}[q_c - q_r] s \quad (79)$$

The low-level PI control action in this case of flexible-joint robots would typically take the form

$$u = -K_P(\dot{\theta} - \dot{q}_c) - K_I(\theta - q_c). \quad (80)$$

Substituting (80) into the second equation of (74) with some further manipulations gives

$$\begin{aligned} D_r(\ddot{\theta} - \ddot{q}) + B_r(\dot{\theta} - \dot{q}) \\ = -K^*(\dot{\theta} - \dot{q}_c) - K K_I(\theta - q_c) \\ - D_r\ddot{q} - B_r\dot{q} - K_s(\theta - q) \end{aligned} \quad (81)$$

and the above equation can further be written as

$$\begin{aligned} D_r(\ddot{\theta} - \ddot{q}) + (B_r + K^*)(\dot{\theta} - \dot{q}) + [(K_s + K K_I)K_s^{-1}]K_s(\theta - q) \\ = -K^*(\dot{q} - \dot{q}_c) - K K_I(q - q_c) - D_r\ddot{q} - B_r\dot{q}. \end{aligned} \quad (82)$$

As the fast dynamics becomes settled, i.e., $K_s(\theta - q)$ is quasi-constant, we obtain that

$$\begin{aligned} K_s(\theta - q) &= -K_s(K_s + K K_I)^{-1} \left\{ K^*(\dot{q} - \dot{q}_c) \right. \\ &\quad \left. + K K_I(q - q_c) + D_r\ddot{q} + B_r\dot{q} \right\} \end{aligned} \quad (83)$$

and thus the slow dynamics becomes

$$\begin{aligned} [M_0(q) + K_s^* D_r] \ddot{q} + C(q, \dot{q}) \dot{q} + (B + K_s^* B_r) \dot{q} + g(q) \\ = -K_s^* K^* [(\dot{q} - \dot{q}_c) + K_I(q - q_c)] \end{aligned} \quad (84)$$

where $K_s^* = K_s(K_s + K K_I)^{-1}$. The fast/slow-dynamics-based analysis given above is based on [10], [43], and one can rigorously obtain the stability and convergence of the system by following similar arguments as in [10], [43].

Remark 8: Different from the rigid robot case, the actual value of the scale parameter now satisfies $\text{diag}[w] = K_s^* K^*$. Part of the low-level integral action in (80) $-K_I(\theta - q)$ is the same as the relative position feedback in [43] and its effect is to increase the joint stiffness, providing the possibility of applying the control to manipulators with a relatively low joint stiffness [43].

Remark 9: It is interesting to note that the joint velocity and position commands in the flexible joint case remains the same as the rigid joint case. This provides a good understanding and more importantly an effective justification of why most results derived in the case of rigid robots are generally applicable to (not justified in the previous literature though) practical robotic systems with inner/output loop structure (e.g., most industrial/commercial robotic systems),

even without the need of any modification (in practice, any robot has certain joint flexibility). In fact, the relative damping suggested in [10] is naturally included as applying the scaled-dynamic-compensation versions of most control schemes valid for rigid robots to (flexible-joint) robots in practice. More remarks in terms of the roles of the rotor inertias and joint stiffness are presented in the later simulation.

One may also be interested in deriving a composite adaptive version of the adaptive scheme for flexible-joint manipulators and it shall be feasible by using similar techniques as those for rigid manipulators.

D. Further Discussions

Here, we take several standard adaptive robot control schemes for illustrating how the scaled dynamic compensation makes them to be qualified adaptive outer loop schemes and further the possible applications to robotic systems with an inner/outer loop structure. It seems hopeful that most adaptive robot control schemes in the literature can be reshaped to be adaptive outer loop schemes by accommodating such modifications.

The inner/outer controller structure basically performs the inner joint servoing much faster and the outer loop relatively slower, and thus the scaled dynamic compensation is actually exerted at a quite lower updating cycle. In the case of fast operating process, this would result in degrading of the performance and even instability at certain extreme cases. The main objective of the study and results presented here is to provide the possibility of exerting dynamic compensation (feedforward) even in the standard setting of industrial robotic systems, of course, under the limit of the operation speed. Once upon a while, direct-drive robots are believed to be promising in taking over the role of the standard robots using gear reduction in that direct-drive robots are much efficient and less influenced by friction and backlash, etc. But this hope advances not so favorably, especially in applications, and the reasons may perhaps be the following:

- The torque output of direct-drive robots is small and large torque output would require large and heavy joint motors, which, however, are significantly constrained by the weight limit of the manipulator;
- direct-drive robots, as is typically expected, are torque-based, but torque-based design is relatively risky and not so reliable since all factors are taken into account at the same time and in addition the communication constraint presents a limit of the coupling torque exerting cycle.

These unfavorable factors concerning torque-based design and direct-drive robots give rise to the welcome of the inner/outer loop structure in most practical robotic applications and this may still be going in the future. A very recent example is Robonaut 2 [45] which uses harmonic gear transmission instead of the direct-drive configuration, and the feedforward is shown to be necessary to improve the control accuracy as well as the system response within the range of the torque limit. In this specific example, the joint torque control loop is open just for admitting the injection of feedforward or dynamic control action, but from a long run and for promoting the large-scale production and decreasing the cost, the inner/outer loop structure with the joint control loop sealed may perhaps be more desirable.

V. SIMULATION RESULTS

A. Task-Space Adaptive Control

Consider a three-DOF manipulator with a tool, as is shown in Fig. 2. Its physical parameters are given in Table I with the labels 1, 2, 3, and E denoting link 1, 2, 3, and the tool, respectively, and the diagonal rotor inertia matrix (seen from the link side) $D_r =$

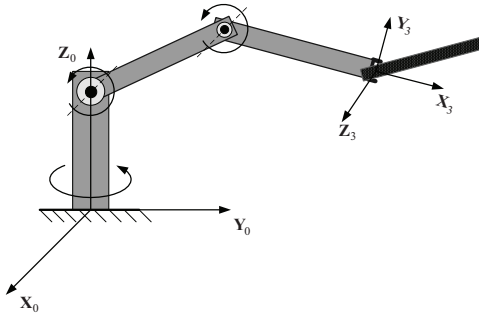


Fig. 2. Three-DOF manipulator.

TABLE I
PHYSICAL PARAMETERS OF THE MANIPULATOR

| i -th body | m_i (kg) | $I_{C,i}^{xx}, I_{C,i}^{yy}, I_{C,i}^{zz}$ (kg · m ²) | l_i (m) | $l_{C,i}$ (m) |
|--------------|------------|---|-----------|---------------|
| 1 | 1.6000 | 0.4320, 0.0720, 0.4320 | 1.8000 | 0.9000 |
| 2 | 0.6000 | 0.0054, 0.1620, 0.1620 | 1.8000 | 0.9000 |
| 3 | 0.6000 | 0.0054, 0.1620, 0.1620 | 1.8000 | 0.9000 |
| E | 0.8000 | 0.0032, 0.0960, 0.0960 | 1.2000 | 0.6000 |

$\text{diag}[0.6, 0.3, 0.1]$. The diagonal matrix B and K are set as $B = \text{diag}[0.20, 0.15, 0.10]$ and $K = \text{diag}[60.0, 30.0, 10.0]$, respectively. The angle about the axis Z_3 between the tool and the third link is $\delta = 30$ deg. The inner joint servoing loop with a PI velocity controller (the case of PID position controller is considered in Sec. V-D) is operated at a high-rate cycle with the sampling period being 0.5 ms, and the outer loop is operated at a low-rate cycle with the sampling period being 20 ms. The gains of the low-level PI controller are set as $K_P = 30.0I_3^1$ and $K_I = 15.0I_3$, and this means that the effective PI gains are $K_P^* = \text{diag}[1800.0, 900.0, 300.0]$ and $K_I^* = \text{diag}[900.0, 450.0, 150.0]$.

1) *Regulation problem:* We first perform the simulations of the system under the filter-based and observer-based task-space regulation schemes. The manipulator starts at the configuration $q(0) = [\pi/6, \pi/3, -5\pi/6]^T$ and the corresponding task-space position is $x(0) = [-0.7500, 1.2990, 0.5196]^T$. The desired task-space position is set as $x_d = [-1.0, 2.0, 0.8]^T$. In the case of using the filter-based scheme, the controller parameters are set as $K_1 = 60.0I_3$, $K_2 = 2.0I_3$, $\alpha = 2.0$, $\Gamma_k = 20.0I_3$, $\Lambda = 0.001I_3$, $\Gamma_d = 0.006I_{15}$, and $\Lambda_I = 100.0I_3$. The initial values of the parameter estimates are chosen as $\hat{a}_k(0) = [3.0, 5.0, 2.0]^T$, $\hat{w}(0) = 0_3$, $\hat{a}_d(0) = 0_{15}$, and $\hat{w}_I(0) = [1, 1, 1]^T$. Simulation results are shown in Fig. 3, Fig. 4, and Fig. 5, which, respectively, give the task-space position errors, the scale parameter estimates, and the estimate of w_I . In the case of using the observer-based scheme, the controller parameters β and γ are determined as $\beta = 1.0$ and $\gamma = 1.0$, which obviously satisfy the condition (30), and the other controller parameters and the initial parameter estimates are chosen to be the same as those of the filter-based scheme. The task-space position error, the scale parameter estimates, and the estimate of w_I are shown in Fig. 6, Fig. 7, and Fig. 8, respectively.

2) *Tracking problem:* Let us now consider the case of using the observer-based tracking controller given by (23), (12), (21), (24), (25), (16), and (17). The desired task-space trajectory is given as $x_d = [-1.0500 + 0.3 \cos(\pi t/3), 1.2990 + 0.3 \sin(\pi t/3), 0.5196 + 0.3 \sin(\pi t/3)]^T$. The initial configuration of the manipulator is set to be the same as the above. The controller parameters are chosen as $\beta = 0.8$, $\gamma = 0.8$, $\Gamma_k = 200.0I_3$, $\Lambda = 6.0I_3$, $\Gamma_d = 27.0I_{15}$,

¹ I_ℓ denotes the $\ell \times \ell$ identity matrix, $\ell = 2, 3, \dots$

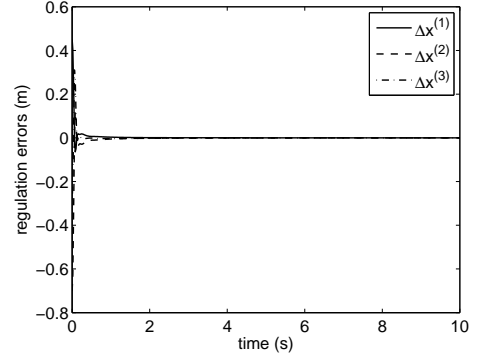


Fig. 3. Task-space position errors (filter-based control).

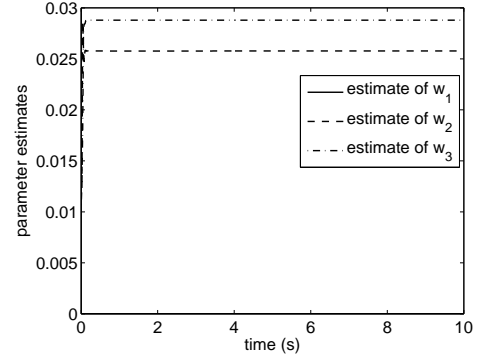


Fig. 4. Scale parameter estimates (filter-based control).

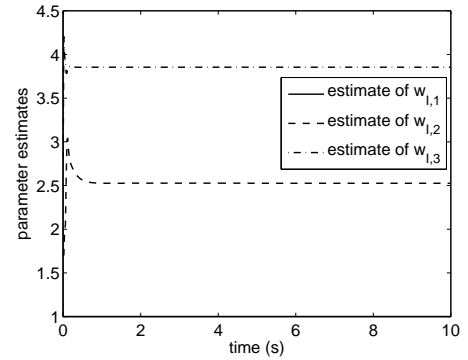
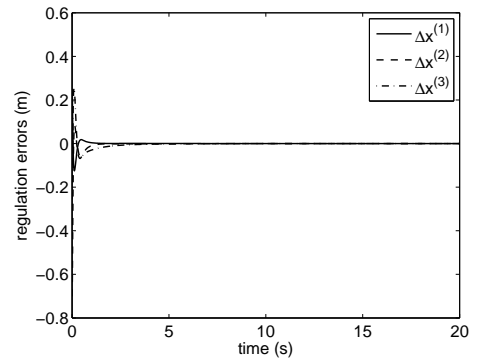
Fig. 5. Estimate of w_I (filter-based control).

Fig. 6. Task-space position errors (observer-based control).

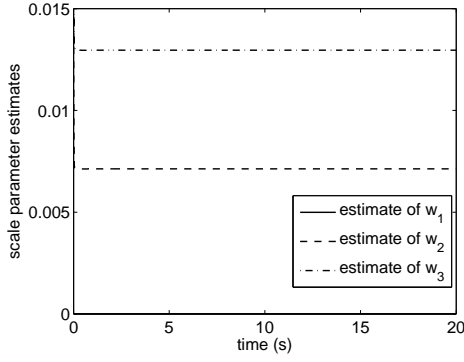


Fig. 7. Scale parameter estimates (observer-based control).

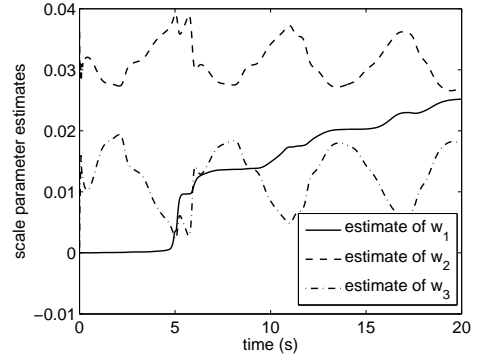
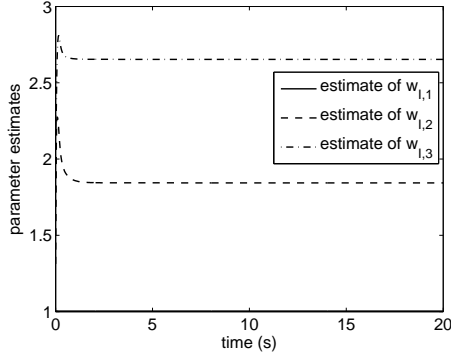
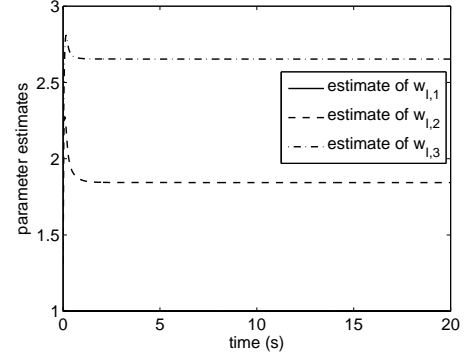


Fig. 10. Scale parameter estimates (observer-based tracking control).

Fig. 8. Estimate of w_I (observer-based control).Fig. 11. Estimate of w_I (observer-based tracking control).

and $\Lambda_I = 100.0I_3$. The task-space position tracking errors, the scale parameter estimates, and the estimate of w_I are shown in Fig. 9, Fig. 10, and Fig. 11, respectively. The gains are increased, in comparison with the the case of regulation, and this is feasible since in the tracking problem here, the desired trajectory starts at the current position of the manipulator.

B. Joint-Space Adaptive Control

Consider first the outer loop version of the direct adaptive controller proposed by Slotine and Li with the controller parameters being chosen as $\bar{\alpha} = 2.0$, $\Lambda = 0.5I_3$, $\Gamma_d = 0.5I_{15}$, and $\Lambda_I = 100.0I_3$. The desired joint trajectory is set as $q_d = 36[(1 - \cos \pi t), \sin \pi t, \sin \pi t]^T$ deg. The initial parameter estimates are chosen as $\hat{w}(0) = 0_3$, $\hat{a}_d(0) = 0_{15}$, and $\hat{w}_I(0) = [1.0, 1.0, 1.0]^T$.

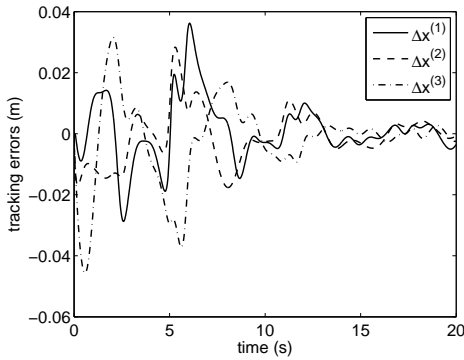


Fig. 9. Task-space position tracking errors (observer-based tracking control).

The joint position tracking errors and parameter estimates are shown in Fig. 12, Fig. 13, and Fig. 14.

We next consider the case of using the composite adaptation in Sec. IV-B with the controller parameters γ_0 and λ_f being chosen as $\gamma_0 = 0.3$ and $\lambda_f = 1.0$ and the other controller parameters the same as those of the direct adaptive controller. The simulation results are shown in Fig. 15, Fig. 16, and Fig. 17, and in comparison with Fig. 12, Fig. 13, and Fig. 14, we see smoother tracking errors and parameter estimates as well as the improved convergence of the tracking errors.

C. Joint-Space Adaptive Control Considering Joint Flexibility

The joint stiffness matrix K_s is set as $K_s = 10^6 \times \text{diag}[6.0, 3.0, 1.0]$ and the diagonal matrix B_r is set as $B_r =$

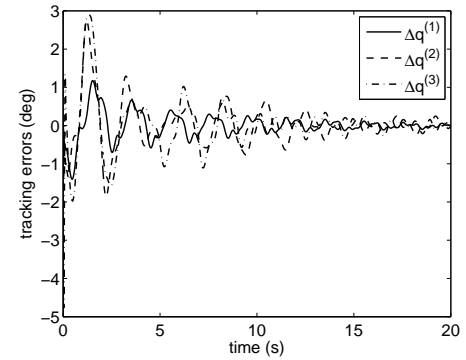


Fig. 12. Joint position tracking errors (direct adaptive controller).

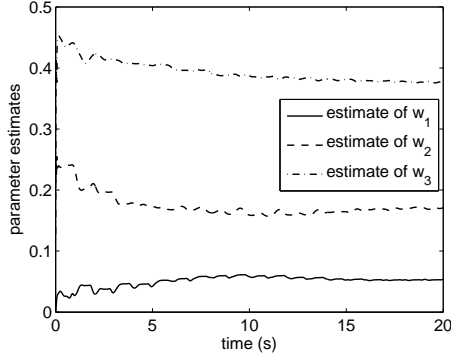


Fig. 13. Scale parameter estimates (direct adaptive controller).

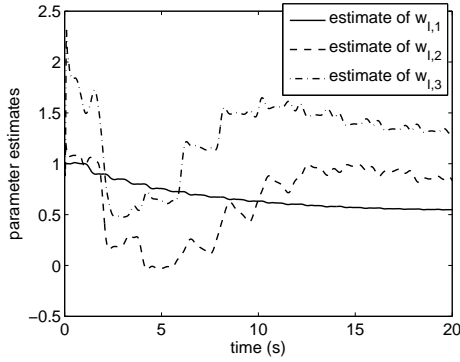
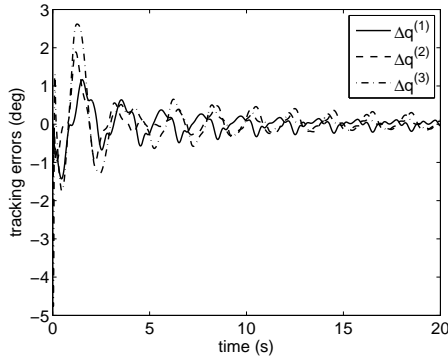
Fig. 14. Estimate of w_I (direct adaptive controller).

Fig. 15. Joint position tracking errors (composite adaptive controller).

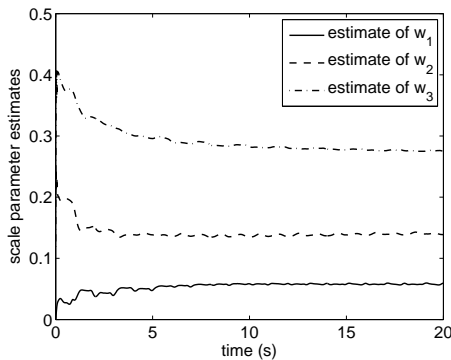
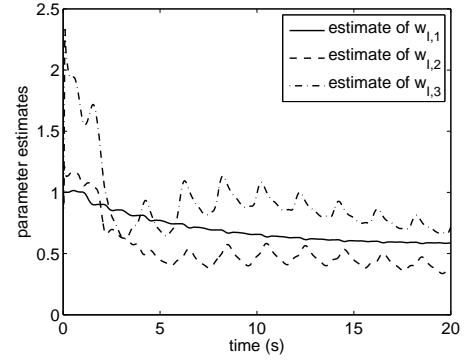


Fig. 16. Scale parameter estimates (composite adaptive controller).

Fig. 17. Estimate of w_I (composite adaptive controller).

$\text{diag}[0.30, 0.20, 0.15]$. The controller parameters are chosen to be the same as the rigid manipulator case except that the adaptation gain Λ_I is reduced to $\Lambda_I = 60.0I_3$. The simulation results are shown in Fig. 18, and we see that the performance is comparable with the rigid manipulator case. But one may need to be cautious about the choice of the rotor inertias, and if the rotor inertias are too small [compared with the manipulator inertia matrix due to the link motion, i.e., $M_0(q)$ in (74)], it is hard to choose a group of controller parameters that can stabilize the system. This is understandable as we recall the standard practice in terms of the design of the motor inertia, i.e., in the case that the motor inertia is strikingly smaller than the load inertia, the whole system would be quite difficult to stabilize and the use of advanced control algorithms does not help much. In particular, we perform a simulation for the case of reduced joint stiffness matrix, i.e., setting K_s to be $K_s = 10^4 \times \text{diag}[6.0, 3.0, 1.0]$ with the rotor inertias remaining unchanged. In addition, as the joint becomes more flexible, it is hard for the manipulator to track a fast time-varying trajectory, and therefore we slow down the evolution of the desired trajectory as $q_d = 36[1 - \cos(\pi t/3), \sin(\pi t/3), \sin(\pi t/3)]^T$ deg. The joint tracking errors are shown in Fig. 19. But as we reduce the rotor inertias to, e.g., 50% of the original, it is very difficult to stabilize the system even with the joint stiffness being unchanged (relatively high). To illustrate the reason behind this phenomenon, we calculate the link inertia matrix $M_0(q)$ at $q = q(0) = 0_3$ and its value is

$$M_0(q) = \begin{bmatrix} 18.9058 & 0 & 0 \\ 0 & 18.9290 & 9.4327 \\ 0 & 9.4327 & 5.1205 \end{bmatrix}.$$

The three eigenvalues of $M_0(q)$ are 0.3352, 18.9058, and 23.7143. This means that the maximum load/rotor inertia ratio reaches $23.7143/0.3 \approx 79$ (happening at the second joint) and such a ratio makes it challenging to stabilize the system. One solution to this problem, as suggested by the standard results in the design of the load/motor ratio, is to increase the joint stiffness, and in other words, larger stiffness allows the specification of larger load/rotor inertia ratio. Fig. 20 shows the joint tracking errors as the stiffness is increased to $K_s = 10^8 \times \text{diag}[6.0, 3.0, 1.0]$ with the desired joint position being still the same as the rigid manipulator case. However, in the simulation, we have to decrease the integration step size so that the stability of the numerical integration can be ensured since the degree of stiffness of the system dynamics is increased. In this particular case (i.e., increased joint stiffness and decreased rotor inertia), the step size is decreased from 0.5 ms to 0.05 ms.

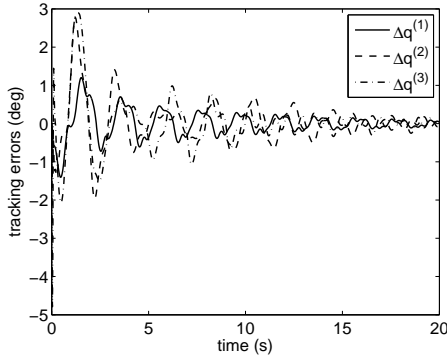


Fig. 18. Joint position tracking errors (flexible joint case).

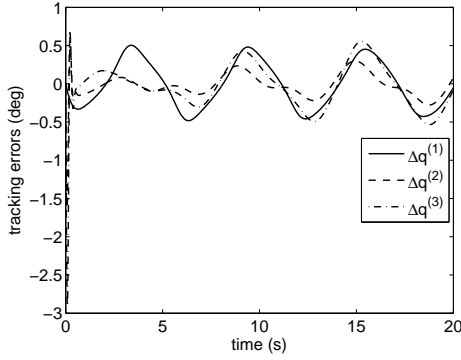


Fig. 19. Joint position tracking errors (reduced joint stiffness).

D. Joint-Space Adaptive Control With an Inner PID Position Controller

The gains of the inner PID position controller is set as $K_D = 30.0I_3$, $K_P = 15.0I_3$, and $K_I = 10.0I_3$. The controller parameters for the joint-space adaptive outer loop controller (which can be developed similarly to the one in Sec. III-D) are chosen as $\bar{\alpha} = 1.5$, $K_c = 0.8$, $\Gamma_d = 0.5I_{15}$, $\Lambda = 0.5I_3$, $\Lambda_P = 100.0I_3$, and $\Lambda_I = 50.0I_3$. The initial parameter estimates are chosen as $\hat{a}_d(0) = 0_{15}$, $\hat{w}(0) = 0_3$, $\hat{w}_P(0) = [1.0, 1.0, 1.0]^T$, and $\hat{w}_I(0) = [1.0, 1.0, 1.0]^T$. The desired trajectory is set to be the same as the case of an inner PI velocity controller. The joint position tracking errors are shown in Fig. 21, which is comparable with the case of an inner PI velocity controller (Fig. 12). Interestingly, no unstable phenomenon is observed even with very fast adaptation to \mathcal{K}_P and \mathcal{K}_I although

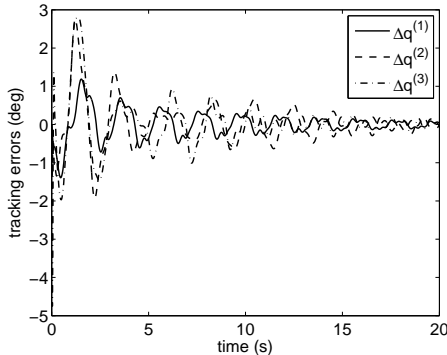


Fig. 20. Joint position tracking errors (increased joint stiffness and decreased rotor inertias).

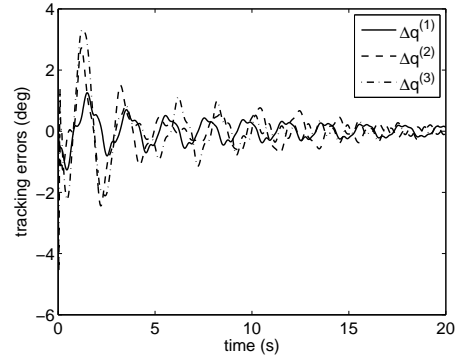


Fig. 21. Joint position tracking errors (adaptive outer loop controller with an inner PID position controller).

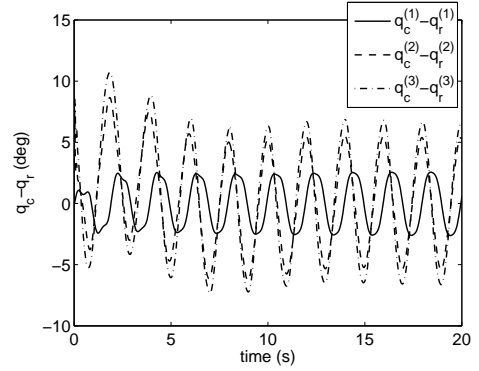


Fig. 22. $q_c - q_r$ (adaptive outer loop controller with an inner PID position controller).

it is currently still challenging to rigorously ensure the uniform exponential stability of (59), and the evolution of $q_c - q_r$ is plotted in Fig. 22. The quantity $q_c - q_r$ (which is apparently bounded based on the data shown in Fig. 22) characterizes the injected dynamic compensation of the proposed controller.

E. Further Remarks

One key issue in the above simulations is the choice of controller parameters including those of the low-level PI controller. Different from most theoretical results in the literature that design control laws at the torque level, the system here actually has two loops with strikingly different updating frequency, namely, the low-rate outer loop and the high-rate inner joint servoing loop. Due to this structure, to guarantee the robustness and performance of the whole system, high gains are specified in the high-rate joint servoing loop while low gains are specified in the low-rate outer loop. We naturally produce a system that consists of two loops with two time-scales and interestingly, it is the system constraint that gives rise to the two-time-scale behavior of the closed-loop system that we cannot modify.

Another issue often involved in practice is the computational efficiency, especially in the case that the number of the DOFs of the manipulator is very large. The typical solution to this problem is the recursive implementation of the adaptive controllers—see, e.g., [32], [46], [47]. The recursive direct adaptive controller as detailed in [32], [46] has the complexity $O(n)$ and the complexity of the recursive composite adaptive controller in [47] is $O(n^2)$, where n denotes the number of the DOFs of the manipulator. We may also note that all the complicated computations of the nonlinear and coupling terms take place in the low-rate outer loop with a powerful computer, and thus

the complexity up to $O(n)$ or $O(n^2)$ is expected to be acceptable.

VI. CONCLUSION

In this paper, we have proposed a dynamic modularity approach to adaptive control of robotic systems with an inner/outer loop structure, and both the task-space and joint-space control are taken into consideration under this framework. The proposed adaptive outer loop controllers take into full account the system dynamic effects while most existing kinematic controllers rely on the ad hoc assumption of fast enough joint servoing loop or the modification of the low-level joint servoing controller to be much more complicated one. From an application perspective, most existing results cannot ensure the stability of the system or convergence of the tracking/regulation error as applied to robotic systems with an inner/outer loop structure (e.g., most commercial/industrial robotic systems) while the proposed adaptive outer loop schemes can guarantee the stability and convergence of the system without the need to modify the low-level joint servoing loop. The goal of the study here is to yield a module robot control system where the adaptive outer loop is user-defined and the inner loop is factory-defined and embedded.

It might be worth discussing the roles of feedback separation in the proposed controllers. Feedback separation is a design objective introduced in the context of Cartesian-space control and visual servoing control of robots with uncertain kinematics (see, e.g., [30], [31]), and the consequence of feedback separation is to reduce the activity of the dynamic compensation action. For instance, the filter-based regulation algorithm in Sec. III-A actually does not achieve feedback separation and thus the scaled dynamic compensation action given in (11) involves an additional term $-\alpha \dot{J}^T(q) \Delta x$ (i.e., a stronger compensation action is required). In contrast, both the observer-based regulation and tracking controllers achieve the feedback separation, benefiting from which, the scaled dynamic compensation action defined in (23) no longer involves additional terms (of course, the controller structure becomes more complex since an observer is introduced). From a control viewpoint, this leads us to reconsider the issue of the cancellation of indefinite terms in the standard backstepping-based control. The cancellation of indefinite terms can lead to a good form of the derivative of the Lyapunov function but often gives rise to potentially decreased robustness and strong coupling between different control loops. The realization of feedback separation may help avoid the unfavorable cancellations of indefinite terms.

Furthermore, the proposed approach may possibly be applicable to other classes of (commercial) mechanical systems (e.g., space robots, mobile robots, or aerial vehicles) that have a hidden torque/force control loop yet admit the design of the velocity (or position) command.

REFERENCES

- [1] M. Aicardi, A. Caiti, G. Cannata, and G. Casalino, "Stability and robustness analysis of a two layered hierarchical architecture for the closed loop control of robots in the operational space," in *Proceedings of the IEEE International Conference on Robotics and Automation*, Nagoya, Japan, 1995, pp. 2771–2778.
- [2] J. Roy and L. L. Whitcomb, "Adaptive force control of position/velocity controlled robots: Theory and experiment," *IEEE Transactions on Robotics and Automation*, vol. 18, no. 2, pp. 121–137, Apr. 2002.
- [3] R. Kelly and J. Moreno, "Manipulator motion control in operational space using joint velocity inner loops," *Automatica*, vol. 41, no. 8, pp. 1423–1432, Aug. 2005.
- [4] K. Camarillo, R. Campa, V. Santibáñez, and J. Moreno-Valenzuela, "Stability analysis of the operational space control for industrial robots using their own joint velocity PI controllers," *Robotica*, vol. 26, no. 6, pp. 729–738, Nov. 2008.
- [5] D. E. Whitney, "Resolved motion rate control of manipulators and human prostheses," *IEEE Transactions on Man-Machine Systems*, vol. MMS-10, no. 2, pp. 47–53, Jun. 1969.
- [6] M. W. Spong and M. Vidyasagar, *Robot Dynamics and Control*. New York: Wiley, 1989.
- [7] M. Grotjahn and B. Heimann, "Model-based feedforward control in industrial robotics," *The International Journal of Robotics Research*, vol. 21, no. 1, pp. 45–60, Jan. 2002.
- [8] F. Sanfilippo, L. I. Hatledal, H. Zhang, M. Fago, and K. Y. Pettersen, "Controlling Kuka industrial robots: Flexible communication interface JOpenShowVar," *IEEE Robotics & Automation Magazine*, vol. 22, no. 4, pp. 96–109, Dec. 2015.
- [9] J.-J. E. Slotine and W. Li, "On the adaptive control of robot manipulators," *The International Journal of Robotics Research*, vol. 6, no. 3, pp. 49–59, Sep. 1987.
- [10] M. W. Spong, "Adaptive control of flexible joint manipulators," *Systems & Control Letters*, vol. 13, no. 1, pp. 15–21, Jul. 1989.
- [11] C. C. Cheah, C. Liu, and J.-J. E. Slotine, "Adaptive Jacobian tracking control of robots with uncertainties in kinematic, dynamic and actuator models," *IEEE Transactions on Automatic Control*, vol. 51, no. 6, pp. 1024–1029, Jun. 2006.
- [12] Y.-H. Liu, H. Wang, C. Wang, and K. K. Lam, "Uncalibrated visual servoing of robots using a depth-independent interaction matrix," *IEEE Transactions on Robotics*, vol. 22, no. 4, pp. 804–817, Aug. 2006.
- [13] W. E. Dixon, "Adaptive regulation of amplitude limited robot manipulators with uncertain kinematics and dynamics," *IEEE Transactions on Automatic Control*, vol. 52, no. 3, pp. 488–493, Mar. 2007.
- [14] H. Wang, "Adaptive visual tracking for robotic systems without image-space velocity measurement," *Automatica*, vol. 55, pp. 294–301, May 2015.
- [15] H. Wang, M. Jiang, W. Chen, and Y.-H. Liu, "Visual servoing of robots with uncalibrated robot and camera parameters," *Mechatronics*, vol. 22, no. 6, pp. 661–668, Sep. 2012.
- [16] M. W. Spong, "On the robust control of robot manipulators," *IEEE Transactions on Automatic Control*, vol. 37, no. 11, pp. 1782–1786, Nov. 1992.
- [17] B. Yao and M. Tomizuka, "Smooth robust adaptive sliding mode control of manipulators with guaranteed transient performance," *Journal of Dynamic Systems, Measurement, and Control*, vol. 118, no. 4, pp. 764–775, Dec. 1996.
- [18] F. Caccavale and P. Chiacchio, "Identification of dynamic parameters and feedforward control for a conventional industrial manipulator," *Control Engineering Practice*, vol. 2, no. 6, pp. 1039–1050, Dec. 1994.
- [19] J. Swevers, W. Verdonck, and J. D. Schutter, "Dynamic model identification for industrial robots," *IEEE Control Systems Magazine*, vol. 27, no. 5, pp. 58–71, Oct. 2007.
- [20] C. C. Cheah, M. Hirano, S. Kawamura, and S. Arimoto, "Approximate Jacobian control for robots with uncertain kinematics and dynamics," *IEEE Transactions on Robotics and Automation*, vol. 19, no. 4, pp. 692–702, Aug. 2003.
- [21] C. C. Cheah, C. Liu, and J.-J. E. Slotine, "Adaptive tracking control for robots with unknown kinematic and dynamic properties," *The International Journal of Robotics Research*, vol. 25, no. 3, pp. 283–296, Mar. 2006.
- [22] X. Liang, H. Wang, W. Chen, and Y.-H. Liu, "Uncalibrated image-based visual servoing of rigid-link electrically driven robotic manipulators," *Asian Journal of Control*, vol. 16, no. 3, pp. 714–728, May 2014.
- [23] H. Wang and Y. Xie, "Prediction error based adaptive Jacobian tracking for free-floating space manipulators," *IEEE Transactions on Aerospace and Electronic Systems*, vol. 48, no. 4, pp. 3207–3221, Oct. 2012.
- [24] H. Wang, Y.-H. Liu, and W. Chen, "Uncalibrated visual tracking control without visual velocity," *IEEE Transactions on Control Systems Technology*, vol. 18, no. 6, pp. 1359–1370, Nov. 2010.
- [25] A. C. Leite, A. R. L. Zachi, F. Lizarralde, and L. Hsu, "Adaptive 3D visual servoing without image velocity measurement for uncertain manipulators," in *18th IFAC World Congress*, Milano, Italy, 2011, pp. 14584–14589.
- [26] H. Wang and Y. Xie, "Observer-based task-space consensus of networked robotic systems: A separation approach," in *Proceedings of the Chinese Control Conference*, Hangzhou, China, 2015, pp. 7604–7609.
- [27] L. E. Weiss, A. C. Sanderson, and C. P. Neuman, "Dynamic sensor-based control of robots with visual feedback," *IEEE Journal of Robotics and Automation*, vol. 3, no. 5, pp. 404–417, Oct. 1987.
- [28] B. Siciliano, "A closed-loop inverse kinematic scheme for on-line joint-based robot control," *Robotica*, vol. 8, no. 3, pp. 231–243, Jul. 1990.
- [29] S. Hutchinson, G. D. Hager, and P. I. Corke, "A tutorial on visual servo

- control,” *IEEE Transactions on Robotics and Automation*, vol. 12, no. 5, pp. 651–670, Oct. 1996.
- [30] H. Wang, “Adaptive control of robot manipulators with uncertain kinematics and dynamics,” *IEEE Transactions on Automatic Control*, DOI: 10.1109/TAC.2016.2575827.
 - [31] —, “Passivity-based adaptive control for visually servoed robotic systems,” *arXiv preprint arXiv:1506.08762*, 2015.
 - [32] G. Niemeyer and J.-J. E. Slotine, “Performance in adaptive manipulator control,” *The International Journal of Robotics Research*, vol. 10, no. 2, pp. 149–161, Apr. 1991.
 - [33] J. J. Craig, *Introduction to Robotics: Mechanics and Control*, 3rd ed. Upper Saddle River, NJ: Prentice-Hall, 2005.
 - [34] M. W. Spong, S. Hutchinson, and M. Vidyasagar, *Robot Modeling and Control*. New York: Wiley, 2006.
 - [35] J.-J. E. Slotine and W. Li, *Applied Nonlinear Control*. Englewood Cliffs, NJ: Prentice-Hall, 1991.
 - [36] C. A. Desoer and M. Vidyasagar, *Feedback Systems: Input-Output Properties*. New York: Academic Press, 1975.
 - [37] M. M. Bridges, D. M. Dawson, and X. Gao, “Adaptive control of rigid-link electrically-driven robots,” in *Proceedings of the IEEE Conference on Decision and Control*, San Antonio, TX, 1993, pp. 159–165.
 - [38] P. A. Ioannou and J. Sun, *Robust Adaptive Control*. Englewood Cliffs, NJ: Prentice-Hall, 1996.
 - [39] H. Berghuis and H. Nijmeijer, “Global regulation of robots using only position measurements,” *Systems & Control Letters*, vol. 21, no. 4, pp. 289–293, Oct. 1993.
 - [40] R. Lozano, B. Brogliato, O. Egeland, and B. Maschke, *Dissipative Systems Analysis and Control: Theory and Applications*. London, U.K.: Springer-Verlag, 2000.
 - [41] C. C. Cheah, C. Liu, and J.-J. E. Slotine, “Adaptive Jacobian vision based control for robots with uncertain depth information,” *Automatica*, vol. 46, no. 7, pp. 1228–1233, Jul. 2010.
 - [42] J.-J. E. Slotine and W. Li, “Composite adaptive control of robot manipulators,” *Automatica*, vol. 25, no. 4, pp. 509–519, Jul. 1989.
 - [43] M. W. Spong, “Adaptive control of flexible joint manipulators: Comments on two papers,” *Automatica*, vol. 31, no. 4, pp. 585–590, Apr. 1995.
 - [44] —, “Modeling and control of elastic joint robots,” *Journal of Dynamic Systems, Measurement, and Control*, vol. 109, no. 4, pp. 310–318, Dec. 1987.
 - [45] T. D. Ahlstrom, M. A. Diftler, R. B. Berka, J. M. Badger, S. Yayathi, A. W. Curtis, and C. A. Joyce, “Robonaut 2 on the International Space Station: Status update and preparations for IVA mobility,” in *AIAA Space Conference and Exposition*, San Diego, CA, 2013, pp. 1–14.
 - [46] H. Wang, “On the recursive implementation of adaptive control for robot manipulators,” in *Chinese Control Conference*, Beijing, China, 2010, pp. 2154–2161.
 - [47] —, “Recursive composite adaptation for robot manipulators,” *Journal of Dynamic Systems, Measurement, and Control*, vol. 135, no. 2, pp. 021 010–1–021 010–8, Mar. 2013.